

## ABSTRACT

LLOYD, KRISTEN HELEN. Clay Mineralogy and Organic Carbon Associations in Two Adjacent Watersheds, New Zealand. (Under the direction of Elana L. Leithold.)

Research conducted on the Waipaoa and Waiapu Rivers on the North Island of New Zealand has recognized and characterized geomorphologic and geochemical processes responsible for the control and delivery of sediment and associated OC to the adjacent margin. Clay mineral compositions from specimens of bedrock, volcanic soils and tephra, suspended river sediment, and recent marine sediments were studied. Identification of the clay minerals was made chiefly by X-ray (XRD), infrared (FTIR), and selective mineral dissolution analyses. Geochemical analyses included organic carbon (OC) concentrations and stable carbon isotopic compositions.

Characteristic clay minerals indicative of bedrock contributions include chlorite and illite. Smectite and kaolinite are also present but in lesser quantities. Soil and tephra mineralogy could not be as easily quantified from x-ray diffraction due to the presence of poorly crystalline minerals (i.e. allophane). FTIR spectrometry proved to be a beneficial tool for the identification of clay minerals in the soil. Allophane and the higher concentration of smectite signify material being derived from the soils and tephra.

Suspended sediment samples collected during moderate to high river flows exhibited a mixed clay mineral composition derived from both bedrock and soil. Within the Waiapu River, bedrock contributions appeared to be greater due to gullyng being the more dominant geomorphologic process. The Waipaoa River showed soil contributions to be as important as rock contributions.

Recent marine sediments off the Waiapu River were similar in composition to the suspended Waiapu River sediment. Spatial variability in clay mineralogy associated with

cross shelf transport reveal chlorite increases at the expense of illite off the Waiapu shelf. A downcore study was conducted on the Waipaoa shelf to examine temporal variability. The sediments in the flood layer and below resemble the river suspension, with smectite being the dominant clay mineral. The presence of allophane in the flood layers suggests a greater contribution from the soil and subsequent rapid burial. The mineralogy of the top layer resembles that seen in the Waiapu, with illite being the dominant clay.

After the clay mineralogy was established, geochemistry was employed to examine contributions from the sources of particulates being delivered to the margin. However, due to the wide range of results, overlap between characteristic isotopic signatures of the sources prevented the successful application of this method.  $\delta^{13}C$  illustrates the mixing of ancient and modern carbon in the rivers and bulk  $\delta^{13}C$  of the rivers is roughly two times greater than the  $\delta^{13}C$  from the rocks. XRD and FTIR results are consistent with and further confirm the mixing of rock and soil particulates in both margins.

Clay Mineralogy and Organic Carbon Associations in Two Adjacent Watersheds, New Zealand

by  
Kristen Helen Lloyd

A thesis submitted to the Graduate Faculty of  
North Carolina State University  
in partial fulfillment of the  
requirements for the Degree of  
Master of Science

Marine, Earth, And Atmospheric Sciences

Raleigh, North Carolina

2007

APPROVED BY:

---

Dr. Dean Hesterberg

---

Dr. Neal Blair

---

Elana Leithold  
Chair of Advisory Committee

## BIOGRAPHY

While I was born in Kansas, I grew up traveling the globe with my family and settled in Fayetteville, NC. My interest in geology started from a young age—I always had my eyes on the ground, was picking up even the smallest pebbles, and loved the outdoors. My last year of high school directed my academic career to geology.

I enrolled at NCSU in 2000 and earned a B.A. in Geology in 2004. After graduation, I decided to further my education at NCSU. In December 2007, I earned a M.S. in Earth Science with a specialization in geology. It has been an adventure and an experience I will cherish and carry with me through life.

## ACKNOWLEDGMENTS

I would like to thank my committee members: Dr. Lonnie Leithold, Dr. Neal Blair and Dr. Dean Hesterberg for their guidance and support in conducting this research. I thank them for their time, knowledge, patience, and perseverance.

To my parents, Howard and Virginia, and sisters, Danielle and Jackie, thank you for all your support and love. You have all been great inspirations in this long journey. If not for your love and support, I would never have been able to accomplish the goals I have set for myself.

I want to thank, Cathy and Laurel, for their assistance in the lab in during this research. I have to commend them on their aid in keeping my sanity throughout this experience. Thank you, Cathy, for providing me with a couch to crash on and always being there through everything. Laurel, without you, we would never have become the Lab Monkeys.

To Remy and Joel, thank you for your help in proofreading, even when you had no clue what I was talking about. I lost count of all the “I don’t know--it’s Greek to me” notations. Joel, thank you for the disc golf breaks that helped me through all the writing.

I wish to acknowledge all my friends for their additional support and for providing activities that allowed all of us to take a break from all the stress and work associated with graduate school.

To the Evil Lab Monkeys, thank you for never completely destroying the lab equipment.

## TABLE OF CONTENTS

|  |    |
|--|----|
| LIST OF TABLES .....   | v  |
| LIST OF FIGURES .....  | vi |
| 1. INTRODUCTION .....  | 1  |
| 1.1 Introduction.....  | 1  |
| 1.2 Site Description: The Waipaoa and Waiapu River Systems.....                | 2  |
| 2. METHODS .....   | 6  |
| 2.1 Sample Collection .....  | 6  |
| 2.2 Sample Preparation and Grain Size Analysis .....                           | 7  |
| 2.3 Dialysis procedures to remove MgCl <sub>2</sub> .....                      | 9  |
| 2.4 Sample Preparation for X-Ray Diffraction .....                             | 9  |
| 2.5 Fourier Transform Infrared Spectrometry .....                              | 11 |
| 2.6 Allophane synthesis .....  | 13 |
| 2.7 Selective Mineral Dissolution and Inductively Coupled Plasma analysis..... | 14 |
| 2.8 Elemental Analysis .....   | 15 |
| 2.9 Stable Carbon Isotopes ( <sup>13</sup> C/ <sup>12</sup> C).....            | 15 |
| 3. RESULTS .....   | 16 |
| 3.1 Grain size Analysis .....  | 16 |
| 3.2 Clay Mineralogy .....  | 17 |
| 3.2.1 Rock Mineralogy .....  | 20 |
| 3.2.2 Soil Mineralogy .....  | 23 |
| 3.2.3 Ash Mineralogy .....   | 29 |
| 3.2.4 River Mineralogy.....  | 33 |
| 3.2.5 Shelf Mineralogy .....   | 37 |
| 3.3 Selective Dissolution Studies .....  | 42 |
| 3.4 Particulate Organic Carbon.....  | 45 |
| 4. DISCUSSION .....  | 50 |
| 5. SUMMARY AND CONCLUSIONS .....   | 56 |
| 6. REFERENCES .....  | 59 |
| 7. APPENDICES .....  | 69 |
| 7.1 Grain size analysis .....  | 70 |
| 7.2 Clay mineral compositions of samples based on Biscaye's method.....        | 71 |
| 7.3 XRD spectra of <2 µm sediment samples for mineralogical analysis .....     | 72 |
| 7.4 FTIR spectra of <2 µm sediment samples for mineralogical analysis.....     | 76 |

## LIST OF TABLES

|   |    |
|---|----|
| Table 2.1 Localities where samples were collected from the Waipaoa and Waiapu watersheds and on the adjacent continental shelf .....                    | 7  |
| Table 2.2 Peak positions used for the identification of clay minerals for XRD .....   | 11 |
| Table 2.3 Weighting factors and equations used for semi-quantification according to Biscaye's method .....  | 11 |
| Table 2.4 Key peaks used in identifying clay minerals in FTIR .....   | 13 |
| Table 3.1 Detailed grain size analysis of two soil profiles collected from within the Waipaoa watershed .....   | 16 |
| Table 3.2 Detailed grain size analysis of Waipaoa River from river suspension during period of high discharge to continental shelf sediments .....      | 17 |
| Table 3.3 Results of Biscaye's method for quantification of clay minerals (based on the Mg <sup>+2</sup> -ethylene glycolated (liquid) treatment) ..... | 19 |
| Table 3.4 of acid ammonium oxalate dissolution of clay samples .....  | 44 |
| Table 3.5 Summarized OC data for bulk and clay (<2 µm) fractions.....   | 49 |

## LIST OF FIGURES

|  |    |
|--|----|
| Figure 1.1 Map of the Waipaoa and Waiapu Catchments .....  | 3  |
| Figure 3.1 Clay compositions of sediment sources (rocks and soil) compared with a short-term sink (the river) and a longer-term sink (the shelf).....        | 20 |
| Figure 3.2 XRD patterns of Mg <sup>+2</sup> -saturated, air dried slides for the Whangai and Tikihore Formations.....  | 21 |
| Figure 3.3 FTIR spectra of <2 µm fraction of the source rocks .....  | 22 |
| Figure 3.4 XRD patterns for Tarndale Road topsoil and ash.....   | 24 |
| Figure 3.5 FTIR spectra for topsoil and an ash layer at the Tarndale Road locality .....   | 26 |
| Figure 3.6 XRD patterns for the topsoil and ash layers from the Te Karaka locality .....   | 27 |
| Figure 3.7 FTIR spectra for the topsoil and ash layers at the Te Karaka site.....  | 28 |
| Figure 3.8 XRD results of the three ash layers (Tarndale and Whakarau Roads, Te Karaka) .....  | 31 |
| Figure 3.9 FTIR spectra of ash layers and synthetic allophane .....  | 32 |
| Figure 3.10 XRD of Waipaoa and Waiapu River suspensions.....   | 34 |
| Figure 3.11 FTIR spectra of Waipaoa and Waiapu River suspensions .....   | 35 |
| Figure 3.12 FTIR spectral comparisons of Waipaoa River to soil and bedrock samples within the catchment.....   | 36 |
| Figure 3.13 XRD results for Poverty Bay (Core U2303) continental shelf sediments off the Waipaoa River.....  | 38 |
| Figure 3.14 FTIR spectra for sediments taken from Core U2303, Poverty Bay, off the Waipaoa River .....   | 39 |
| Figure 3.15 XRD results of sediments taken from cores offshore to the Waiapu River .....   | 40 |
| Figure 3.16 FTIR results of continental shelf sediments adjacent to the Waiapu River .....   | 41 |
| Figure 3.17 Depth and Al:Si relationships from soil and ash profiles from samples collected at the Tarndale and Whakarau Road and Te Karaka localities ..... | 44 |

|  |    |
|--|----|
| Figure 3.18 Ranges of $\delta^{13}\text{C}$ values of bulk and $<2\mu\text{m}$ clay fractions according to sample type ..... | 46 |
| Figure 3.19 OC peaks present in FTIR for the Tarndale Road and Te Karaka topsoils .....                                      | 47 |

# **1. INTRODUCTION**

## **1.1 Introduction**

Most of the particulate organic carbon (POC) delivered by rivers to the oceans is bound to clay-sized mineral grains, and on the continental margins these OC/mineral complexes potentially preserve a record of terrestrial environmental change over time (Keil and Hedges, 1993; Keil et al., 1997; Leithold et al., 2005). Recent investigations in small mountainous watersheds in Taiwan, California, Oregon, and New Zealand indicate that the character of the particle-bound carbon suspended in rivers is governed by the relative importance of erosion processes that deliver rock carbon and soil to channels (Kao and Liu, 1996; Gomez et al., 2003; Leithold et al., 2006). In New Zealand, for example, stable and radiogenic carbon isotopes ( $\delta^{13}\text{C}$ ,  $\Delta^{14}\text{C}$  respectively) have been used to estimate that approximately 50% of the POC discharged from the Waipaoa River and 70% of the POC discharged from the Waiapu River is ancient, rock-derived carbon, with the balance being composed primarily of young, plant-derived OC (Leithold et al., 2006).

The aim of this thesis is to develop an additional tool to test and refine these estimates as a contribution toward determining how human activities and climate change have affected erosion processes in these watersheds over the past thousands of years. In this thesis, the clay mineralogy of rocks, volcanic soils, and ash layers in the Waipaoa and Waiapu watersheds was first examined to establish the mineralogical characteristics of material being delivered to the river channels. River suspensions and continental shelf deposits were then analyzed to see if the different watershed sources could be distinguished. Finally, the concentration and stable isotopic composition of carbon associated with bulk samples and clay-sized grains from these different deposits were assessed.

## **1.2 Site Description: The Waipaoa and Waiapu River Systems**

The Waipaoa and Waiapu catchments on the North Island of New Zealand have some of the highest global erosion rates, and thus are ideal for the investigation of the relationships among erosion processes, clay mineralogy, and POC. The catchments are small in size (2205 km<sup>2</sup> and 1743 km<sup>2</sup>, respectively), located in an active tectonic setting and contain old, highly fractured sedimentary rocks overlain by young volcanic soils. The organic carbon in the watersheds can be characterized as terrestrial and marine ancient rock-derived and modern plant-derived (Gomez et al., 2003b; Leithold et al., 2006).

The physical appearance of these two catchments has changed over their history. Native forests covered much of the landscape, but the clearing of the forests on flat landscapes began with the arrival of Polynesian settlers and agriculture (Glade, 2003). Over the 19<sup>th</sup> and 20<sup>th</sup> centuries, the deforestation and rise of agriculture within the watersheds led to increased weathering rates and increased sediment flux to the continental shelf (Glade, 2003; Gomez et al., 2003a, b). Today, nearly all the Waipaoa catchment has been converted to pastureland and 2.5% of the natural native forest landscape exists today (Gomez et al., 2004a; Owens et al., 2005). The increased weathering has also increased the delivery of POC to the adjacent continental shelf.

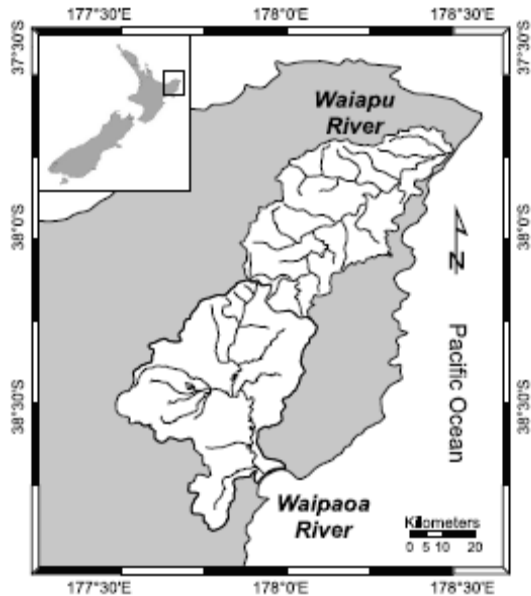


Figure 1.1 Locations of the Waipaoa and Waiapu catchments, North Island, New Zealand. (From Leithold et al., 2006)

The Waipaoa River is categorized as New Zealand's fourth largest river in terms of sediment supply, and it delivers an estimated 15Mt/yr of suspended sediment to Poverty Bay off the East Coast of the North Island (Glade, 2003; Orpin, 2004). With a catchment size of 2205 km<sup>2</sup>, the river drains the eastern flanks of the Raukumara Mountain Range. Much of the watershed is extensively underlain by Cretaceous to early Tertiary calcareous mudstones and argillites interbedded with very fine sandstones of the Whangai and Tikiore Formations (Mazengarb and Speden, 2000; Gomez et al., 2003a, b; Laird et al., 2003). These units are believed to have accumulated in a shallow shelf environment that was swept by frequent storms and periodic tectonic activity (Mazengarb and Speden, 2000; Laird et al., 2003).

While the Waiapu River has a smaller basin size (1743 km<sup>2</sup>), this upland river has been labeled as one of the muddiest rivers in the world. The Waiapu River discharges 35 Mt/yr of sediment on to the continental shelf adjacent to the East Coast of the North Island (Hicks et al., 2000, 2004; Kasai et al., 2005). The geology of the Waiapu catchment is similar

to that of the Waipaoa, with the dominant rocks being from the Whangai and Tikihore Formations (Kasai et al., 2005). The Tikihore Formation consists of interbedded, fine-grained, siliceous sandstones and carbonaceous mudstones (Mazengarb and Speden, 2000). Average annual rainfall for the Waiapu catchment is 2400 mm, which is significantly higher than the 1000-2000 mm for the Waipaoa catchment (Hicks et al., 2000; Reid and Page, 2002; Kasai et al., 2005).

Soils in the Waipaoa and Waiapu catchments have developed on the crushed bedrock and have had episodic contributions of Quaternary volcanic tephra from nearby volcanic centers. The mineralogy of the soil reflects its parent material composition with the inclusion of short range order minerals specifically found within these volcanic soils. Andisols are mainly dark-colored and are marked by presence of volcanic glass, short-range-order minerals (allophane, imogolite, ferrihydrite), low bulk density, high phosphorous-fixing capacity and the accumulation of and capacity to sorb organic matter (Soil Survey Staff, 1999; Ugolini and Dahlgren, 2002; Buol et al., 2003).

Landscape changes over time have led to the production of highly unstable landforms which result in the incision of large gully complexes in the soft bedrock, particularly those rocks with high clay contents (Mazengarb and Speden, 2000). Detailed studies of the effects of land use change on the Waipaoa catchment have documented the flood of sediment from gullies and landslides to Poverty Bay (Glade, 2003; Gomez et al., 2003a, b; Orpin, 2004, Leithold et al., 2006). Studies of gully complex activity have indicated that the complexes can remain active for a period of one to two years after a major storm event (Glade, 2003; Kasai et al., 2005). Whereas gullies are a steady source of rock and soil erosion, shallow landslides involve small, <1m deep planar failures that originate at the soil-bedrock interface

or within the soil profile, thus providing a mixture of sediment from the soil and rocks (Gomez et al., 2004). Episodic storms affect the catchment and can reactivate the gullies and landslides. Winter storms tend to be small and frequent, and landsliding becomes more prevalent with episodic, high intensity storms (DeRose et al., 1998; Hicks et al., 2000; Reid and Page, 2002; Glade, 2003; Gomez et al., 2003 a, b; 2004; Orpin, 2004; Leithold et al., 2006).

The suspended loads of the Waipaoa and Waiapu Rivers contain fine mineral particles (silt and clay) and organic matter that are generated during winter storms, with their highest yields occurring in the winter months (Glade, 2003). Studies have shown that as river flows increase due to storm activity, the concentration of suspended material increases and the percentage of POC decreases (Gomez et al., 2004a). It is within the suspended sediment that the clay-sized fraction ( $<2 \mu\text{m}$ ), which serves an important role in the exchange and preservation of organic matter, is concentrated (Brady and Weil, 2000).

Storm events are responsible for generating large amounts of sediment in the catchment, and they may produce flood layers that are preserved on the continental margins. In recent years, the deposits of one such storm have been recorded and studied in Poverty Bay. In 1988, Cyclone Bola was one of the most intense storms to affect the catchment and has been categorized as a 100-year storm (Kasai et al., 2005). It was responsible for delivering 300 to 900 mm of rainfall over the Waipaoa catchment in a 4-day period (Hicks et al., 2000; Reid and Page, 2002). The immense rainfall totals triggered massive landslides and delivered large amounts of fine-grained material and plant debris to the river channel. Effects of Cyclone Bola were mostly felt in areas covered by pasture, and the contribution of

sediment from gullies did not increase significantly (Kasai et al., 2005). This apparent stabilization of gullies is attributed to the increased reforestation practices since 1938.

## **2. METHODS**

### **2.1 Sample Collection**

Volcanic soil, tephra, rock, river suspension and marine shelf samples were collected over the course of two visits to the North Island between 2003 and 2004. Locations and dates of sampling are given in Table 2.1. Rock samples representative of the dominant lithologies were collected from surface exposures where the exterior surfaces did not show signs of heavy weathering or contamination with debris from plants or soil. Soil pits dug by hand were used to collect soil and ash samples, and a profile description was made. Ash and soil samples collected at various intervals from clearly distinguishable horizons within the profile were then frozen (Table 2.1). River suspensions were collected by lowering a Wildco Beta Plus horizontal water bottle into the river at a depth just below the surface and the samples frozen within a few hours. Later the frozen water samples were allowed to thaw and then centrifuged to concentrate the sediment. The sediment was then frozen until analysis. Continental shelf cores were collected on two separate cruises on the RV Tangaroa in March and May 2001 and the cores were subsectioned. All samples collected were kept frozen until analysis.

Table 2.1 Localities where samples were collected from the Waipaoa and Waiapu watersheds and on the adjacent continental shelf.

| <b>Sample Locality</b>                                     | <b>Sample Collected</b>             | <b>Date Collected (yy/mm/dd)</b> | <b>Geographic Coordinates</b>    | <b>Sample ID</b>                                   |
|--|-------------------------------------|----------------------------------|----------------------------------|--|
| Waipaoa Catchment  | Whangai Formation (mudstone)        | 03/05/13                         | S 38° 21.880'<br>E 177° 35.819'  | WK030513-5   |
| Whakarau Road, Waipaoa Catchment                           | Ash                                 | 03/05/13                         | S 38° 18.872'<br>E 177° 34.185'  | WK030513-7   |
| Waiapu Catchment   | Tikihore Formation (sandstone)      | 03/05/19                         | S 37° 57.856'<br>E 178° 09.943'  | WU030519-2   |
| Waiapu River, Bridge near Ruatoria                         | River Suspension 5.40 m stage       | 03/09/17                         | S 37° 53.695'<br>E 178° 17.734'  | WU030917-5.40                                      |
| Te Karaka; Waipaoa   | Soil and Ash (10, 13, 43 cm)        | 04/06/08                         | S 38° 28.514'<br>E 177° 52.061'  | TK040608-1<br>TK040608-2<br>TK040608-3             |
| Tarndale Road; Waipaoa                                     | Soil and Ash (10, 80 cm)            | 04/06/09                         | S 38° 19.284'<br>E 177° 47.889'  | TD040609-2<br>TD040609-6                           |
| Waipaoa River at Kanakanaia                                | River Suspension 4.83 m stage       | 04/06/30                         | S 38° 27.0012'<br>E 177° 52.009' | WK040630-4.83                                      |
| MC3 Waiapu continental shelf, 43 m water depth             | Continental Shelf Sediment (1-2 cm) | Tangaroa Cruise                  | S 37° 47.882'<br>E 178° 32.904'  | TAN0314-31<br>MC3 1-2 cm                           |
| MC10 Waiapu continental shelf, 117 m water depth           | Continental Shelf Sediment (1-2 cm) | Tangaroa Cruise                  | S 37° 49.387'<br>E 178° 38.394'  | TAN0314-50<br>MC10 1-2 cm                          |
| Poverty Bay, 27 m water depth, offshore from Waipaoa River | Continental Shelf Sediment          | 01/03/25                         | S 38° 45.015'<br>E 178° 01.996'  | U2303 4-6 cm,<br>U2303 18-19 cm,<br>U2303 31-33 cm |

## 2.2 Sample Preparation and Grain Size Analysis

Samples selected from rocks, volcanic soils, river suspensions and shelf cores were used to characterize the sediment being generated and transported through the Waiapu and

Waipaoa catchments. Bulk rock samples were ground with a ceramic mortar and pestle and bulk sediment samples were homogenized with a metal or glass stir rod and approximately 15 to 20 grams was used to separate into clay ( $<2\ \mu\text{m}$ ), medium-fine silt ( $2\text{-}25\ \mu\text{m}$ ), and coarse silt and sand ( $>25\ \mu\text{m}$ ) fractions. The sediment was mixed with deionized water and a dispersant (sodium hexa-metaphosphate,  $1\ \text{g/L}$ ) to prevent flocculation and the solution was shaken on a reciprocating shaker for 1h at 220 rpm. After shaking, the sediment was washed through a  $25\ \mu\text{m}$  stainless steel sieve with deionized water and collected in a 1L graduated cylinder. The remaining sample ( $>25\ \mu\text{m}$ ) that did not pass through the sieve was collected and later frozen. The material that passed through the sieve was further fractionated into medium-fine silt and clay sizes ( $<25\ \mu\text{m}$  and  $<2\ \mu\text{m}$ ) by standard settling techniques utilizing Stokes Law. To measure the percentage of the medium-fine silt fraction  $<25\ \mu\text{m}$  in the sample, the solution was homogenized and 40 mL was withdrawn and centrifuged in a glass tube for 1h at 2500 rpm. After centrifugation, 5 mL of the supernatant was removed by pipette to calculate the amount of dispersant in the sub-sample. To collect the  $<2\ \mu\text{m}$  clay fraction, the mixture in the cylinder was allowed to settle for 19 hr 16 min in a room with a relatively constant temperature of  $17\text{-}18^\circ\text{C}$  and the top 26 cm of the solution was pumped out via a peristaltic pumping system ( $60\ \text{mL/min}$ ). To aid in clay flocculation, 5 mL of a 10% solution of  $\text{MgCl}_2$  were added to the  $<2\ \mu\text{m}$  fraction. The solution was then centrifuged until the clay fraction had settled. Five milliliters of the supernatant was collected and dried to calculate the weight of  $\text{MgCl}_2$  in the  $<2\ \mu\text{m}$  fraction. The  $<2\ \mu\text{m}$  fraction was collected, freeze dried, and kept frozen until further analysis.

### **2.3 Dialysis procedures to remove MgCl<sub>2</sub>**

Spectra/Por 3 Regenerated Cellulose Dialysis Membrane was used to aid in the removal of the added salts in the samples. Pieces of the dialysis tubing were soaked in deionized water for 30 minutes to remove any preservatives. The dried <2 μm clay fraction with MgCl<sub>2</sub> was mixed with deionized water and then added to the tubing and closed off. The tubing was placed in a 1L beaker of deionized water and allowed to sit in a cold room (5°C). The water in the beaker was replaced every 4 to 6h. To check for the presence of salt in solution, a few drops of a 0.1M solution of AgNO<sub>3</sub> (1.7 g AgNO<sub>3</sub> crystals:98 ml DI) were added to the dialysate. Salts were detected by the formation of a white AgCl precipitate, and when the AgCl was evident, the water in the beaker was replaced with deionized water and the dialysis procedure continued. This test for salts was repeated until Cl<sup>-</sup> could no longer be detected in the dialysate. The dialyzed <2 μm clay fraction was then transferred into beakers, freeze dried, and kept frozen until analysis.

## **CLAY MINERALOGY**

### **2.4 Sample Preparation for X-Ray Diffraction**

X-ray diffractometry (XRD) was used in conjunction with Fourier Transform Infrared Spectrometry (FTIR) to characterize clay minerals present in the suite of terrestrial soils, volcanic tephra, bedrock and marine sediments from the Waiapu and Waipaoa watersheds and adjacent continental shelf. The utilization of XRD is advantageous for the identification of solid materials with crystalline (long-range order) structures, particularly crystalline clay minerals.

To identify phyllosilicate clay minerals present in the  $<2 \mu\text{m}$  fraction, samples were prepared with saturation treatments of magnesium or potassium according to Dixon and White (1997). Two solutions of 0.5 M  $\text{MgCl}_2$  and 1 M  $\text{KCl}$  were prepared for saturation treatments of the clays. For each treatment, 25 mL of solution was added to approximately 15 mg of each clay fraction in 50 ml polyethylene centrifuge tubes. The tubes were then centrifuged for 15 min at 2500 rpm. The supernatant was decanted off, and the process repeated two additional times to ensure thorough saturation with magnesium or potassium. The clay samples were then rinsed with deionized water until the particles stayed dispersed and no additional salts could be detected in the solution. The absence of salts was verified by the absence of  $\text{Cl}^-$  determined by adding a few drops of  $\text{AgNO}_3$  to the solution. The slurry from each treatment was pipetted onto glass microscope slides and air dried.

All samples were analyzed on a Rigaku D/Max B Cu K-alpha X-Ray Diffractometer at 35 mA and 30 kV. Analyses were conducted using the step scan mode with a scan range of 3 to  $35^\circ 2\theta$ , a step size of  $0.5^\circ 2\theta$  and a 1 s dwell time.

After the initial analysis, the  $\text{K}^+$ -saturated clay slides were heated to  $300^\circ\text{C}$  for six hours and reanalyzed to check for the presence of gibbsite and hydroxyl-interlayered minerals. The slides were heated for a second time to  $550^\circ\text{C}$  and reanalyzed to distinguish the differences between kaolinite and chlorite because the structure of kaolinite decompose at this temperature (Moore and Reynolds, 1997). To check for the presence of expansive (smectitic) minerals, such as montmorillonite, the  $\text{Mg}^{+2}$ -saturated clay samples were saturated with liquid ethylene glycol directly on the slides. Following the method summarized by Mosser-Ruck et al. (2005), a few drops of the ethylene glycol were applied to the edge of the clay and allowed to diffuse into the slide until the slide was visibly moist.

Excess ethylene glycol was removed by gently pressing an absorbent laboratory tissue on the slide. The glycol-saturated slides were then analyzed. Table 2.2 summarizes XRD peaks for common silicate minerals.

Table 2.2 Peak positions used for the identification of clay minerals for XRD (after Moore and Reynolds, 1997).

| Mineral   | Peak Position (nm)   |
|-----------|----------------------|
| Chlorite  | 1.4, 0.710, 0.354    |
| Illite    | 1.00, 0.50, 0.334    |
| Kaolinite | 0.710, 0.358         |
| Smectite  | 1.4, 1.0, 0.5, 0.375 |
| Quartz    | 0.426, 0.334         |

Biscaye's method (1965) was utilized to semi-quantitatively estimate the proportions of different clay minerals in the samples, with diagnostic XRD peak weighing factors given in Table 2.3. To facilitate comparisons between samples, the intensity scale was normalized to 1,000 counts using the Jade 6.0 software.

Table 2.3 Weighting factors and equations used for semi-quantification according to Biscaye's method.

| Mineral   | Weighting Factor of mineral peak | Equation for calculating mineral %     |
|-----------|----------------------------------|--|
| Smectite  | 1 x 17Å                          | $(S \times 100) / (S + 4I + 2K + 2C)$  |
| Illite    | 4 x 10Å                          | $(4I \times 100) / (S + 4I + 2K + 2C)$ |
| Kaolinite | 2 x (7Å / 3.58Å)                 | $(2K \times 100) / (S + 4I + 2K + 2C)$ |
| Chlorite  | 2 x (7Å / 3.54Å)                 | $(2C \times 100) / (S + 4I + 2K + 2C)$ |

## 2.5 Fourier Transform Infrared Spectrometry

Fourier Transform Infrared Spectroscopy (FTIR) is a useful tool in the characterization of the clay mineralogy because of its ability to identify well-structured and crystalline minerals as well as poorly crystalline or non-crystalline solids, such as allophane and imogolite. X-ray "amorphous" solids absorb infrared radiation as strongly as crystalline

minerals, and therefore, their presence within a mixture of crystalline minerals is more detectable from infrared spectra than from X-ray diffraction patterns (Farmer and Russell, 1966). Thus the combination of FTIR and XRD results provided a better identification of the clay mineralogy for the Waipaoa and Waiapu catchments.

The <2  $\mu\text{m}$  clay fraction was freeze dried overnight to remove any excess moisture within the sample. Approximately 0.5 to 1.5 mg of sample and 80 to 100 mg of crystalline KBr were weighed out and ground in an agate mortar until thoroughly homogenized. The powder was pressed into a disc and analyzed on a Nicolet Impact 400D FTIR spectrometer with scans conducted at a range of 4000 to 400  $\text{cm}^{-1}$ . FTIR works by infrared radiation passing through pressed discs of the powdered mineral sample suspended in KBr. Infrared radiation produces lattice vibrations between bonded atoms within the mineral, including stretching and bending vibrations. Different molecular structures absorb infrared radiation at different energies and produce characteristic absorption peaks unique to the minerals present in the sample.

After a sample spectrum was collected, the resulting spectrum scale was normalized to the highest peak in the spectrum using Omnic software. This was performed to facilitate comparisons between the samples. Mineral identification relied on comparisons to published spectra (Russell et al., 1981; Wilson, 1994; Madejová and Komadel, 2001; Ohashi et al., 2002; Post and Borer, 2002; Pironon et al., 2003; Certini et al., 2006), and characteristic peaks for various minerals and short-range order solids are given in Table 2.4.

Table 2.4 Key peaks used in identifying clay minerals in FTIR.

| Clay Mineral      | Peak Position (cm <sup>-1</sup> )                  |
|-------------------|--|
| Kaolinite         | 3697, 3669, 3652, 3620, 1036, 1016, 912, 540       |
| Illite            | 3620, 916, 831, 695, 527                           |
| Smectite          | 3620, 1088, 1008, 916, 798, 525, 467               |
| Chlorite          | 3563, 3432, 1082, 668, 520, 431                    |
| Illite-Smectite   | 1031, 840, 755, 524, 469                           |
| Chlorite-Smectite | 3676, 3567, 1088, 669, 463                         |
| Allophane         | 3530, 3420, 971, 962, 874, 793, 668, 581, 509, 428 |
| Gibbsite          | 3620, 3463, 581, 505, 448                          |
| Quartz            | 798, 779   |

References: Russell et al., 1981; Wilson, 1994; Madejová and Komadel, 2001; Ohashi et al., 2002; Post and Borer, 2002; Pironon et al., 2003; Certini et al., 2006

## 2.6 Allophane synthesis

As stated, infrared spectrometry is more useful than XRD for the identification of allophane because of the short-range order of this solid. However, it is important to note that the signature XRD and IR peaks for allophane are broad and can be obscured by other phyllosilicate minerals (Parfitt, 1990).

Two allophane standards were synthesized to aid in the identification of allophane in the Waipaoa samples. The synthetic allophane was mixed with source clay standards from the Clay Minerals Society to examine the sensitivity of the detection by FTIR. Observations from these tests were used to help in the identification of allophane peaks that might be present or muted in the FTIR spectra by other minerals.

Procedures for the synthesis of allophane from high concentrate solutions follow Ohashi et al (2005). Two synthetic allophane standards were created from aqueous solutions of Na<sub>4</sub>SiO<sub>4</sub> and AlCl<sub>3</sub>\*6H<sub>2</sub>O at concentrations of 30 and 100 mmol/L. Crystals of Na<sub>4</sub>SiO<sub>4</sub> and AlCl<sub>3</sub>\*6H<sub>2</sub>O were dissolved in 500 mL of deionized water. The two solutions were then

combined to produce allophane with a 0.75 ratio of Si:Al and centrifuged for two hours at 2700 rpm in Teflon bottles. The supernatant was then carefully decanted so as not to suspend the precipitated gel that formed at the bottom of the bottles. For the removal of salts in solution, deionized water was added to the Teflon bottles and centrifuged. This procedure was repeated until  $\text{Cl}^-$  could no longer be detected with  $\text{AgNO}_3$ . After centrifuging and decanting most of the supernatant, the remaining solution and precipitate were left in the sealed bottle and allowed to heat in a blower-equipped oven at  $90^\circ\text{C}$  for 48 hours. The precipitate and supernatant were then put into a drying oven to allow the supernatant to evaporate, leaving the synthetic allophane.

## **2.7 Selective Mineral Dissolution and Inductively Coupled Plasma analysis**

Many studies have used selective mineral dissolution techniques to estimate the amount of allophane present in volcanic soils (Russell et al., 1981; Parfitt et al., 1983; Lowe, 1986; Parfitt et al., 1990). Following techniques described by Carter (1993), acid-oxalate extractions were used to selectively dissolve the Al and Si in short-range ordered minerals. The samples were treated with 10 mL of a 0.2 M solution of acid ammonium oxalate and shaken in the dark for four hours. After shaking, the tubes were centrifuged for 20 minutes at 2500 rpm and the supernatant was decanted and analyzed for acid oxalate extractable Al, Fe and Si on a Perkin-Elmer model Optima 2000DV, NCSU Analytical Services Lab in Soil Science by standard inductively coupled plasma optical emission spectrometry (ICP-OES) procedures.

To calculate the amount of Al and Si extracted from the samples, the following formula was used:

$$\% \text{ Al, Si} = \frac{\text{concentration } (\mu\text{g/mL}) \text{ in final solution} * \text{extractant volume (mL)} * \text{dilution factor} * 100}{\text{Sample wt (mg)} * 1000} \quad \text{Eqn 1.}$$

## 2.8 Elemental Analysis

Bulk and <2  $\mu\text{m}$  fractions of each sample were prepared for determination of their organic carbon (OC) and nitrogen content. The samples were first acidified with aqueous 4N HCl for two to four days to dissolve any inorganic carbon. After acidification, the samples were dried *in vacuo* at room temperature. To measure the amount of OC and nitrogen, the samples were loaded into tin boats and analyzed on a Thermo Finnigan Flash EA1112 elemental analyzer.

## 2.9 Stable Carbon Isotopes ( $^{13}\text{C}/^{12}\text{C}$ )

The  $\text{CO}_2$  produced from the combustion of the organic matter in the EA was collected cryogenically (Blair and Carter, 1992) and initially analyzed for carbon isotopic ratios using a Delta V IRMS set up on a standard dual inlet, where samples were compared to a reference gas (NBS-3). During the course of this research, the connection between the EA and the mass spectrometer was changed to allow for sample analysis utilizing the continuous flow method. Some samples were analyzed a second time using the continuous flow method and the  $\delta^{13}\text{C}$  results were comparable.

### **3. RESULTS**

#### **3.1 Grain Size Analysis**

Two soil profiles examined at the Tarndale Road and Te Karaka localities consisted of dark topsoil ranging from 5 to 10 cm thick overlaying lighter subsoils, with identifiable white to tan volcanic ash layers at 10 to 13 cm depth and 75 to 93 cm depth, Te Karaka and Tarndale respectively. Pumice fragments were identified closer to the surface, and mottling found at greater depth in the Te Karaka profile suggests the weathering of pumice. A decrease in sand concentration can be seen with increasing depth (Table 3.3). Additionally, increases in silt and clay fractions with depth are attributed to transformations and translocations of minerals and material within the soil.

Table 3.1 Detailed grain size analyses of two soil profiles collected from within the Waipaoa watershed.

|  | <b>Profile 1<br/>Tarndale</b> |              | <b>Profile 2<br/>Te Karaka</b> |              |              |
|--|-------------------------------|--------------|--------------------------------|--------------|--------------|
|  | <b>10 cm</b>                  | <b>80 cm</b> | <b>10 cm</b>                   | <b>13 cm</b> | <b>43 cm</b> |
| <b>% &gt;25 <math>\mu\text{m}</math></b> | 75.90                         | 72.04        | 55.92                          | 39.65        | 22.44        |
| <b>% 2-25<math>\mu\text{m}</math></b>    | 23.36                         | 26.25        | 42.25                          | 53.88        | 56.95        |
| <b>% &lt;2 <math>\mu\text{m}</math></b>  | 0.74                          | 1.71         | 1.83                           | 6.47         | 20.61        |

During the winter months, there was an increased sediment delivery to the Waipaoa River via material being generated by the deeply incised gullies and shallow landslides during high intensity storms. There is an increase in the amount of fine-grained material being transported by the river during times of high discharge, and from one suspension sampled from the Waipaoa River, approximately 92% of the suspended load consisted of silt- and clay-sized (2-25 $\mu\text{m}$ ) material. The sampled Waipaoa suspension exhibited a similar percentage of silt- and clay-sized material (93%).

The shelf sediments from the Poverty Bay core U2303 (Table 3.2) at 27 m water depth were subdivided into three subsamples marking “normal” shelf deposition and a flood layer (Brackley, 2006). The two samples representing “normal” shelf deposition at intervals of 4-6 cm and 31-33 cm were composed of approximately 80% sand. A subsample (18-19 cm) taken from the center of a 10 cm thick flood layer is thought to have been a result of Cyclone Bola (Brackley, 2006). In 1988, the storm triggered massive landslides throughout the catchment and increased the amount of the fine fraction being transported as suspended sediment carried by the river (Kasai et al., 2005). This flood layer is composed of nearly 95% silt and clay sediment (Table 3.2), while the two samples taken from above and below the flood layer are composed of less than 20% silt and clay fractions.

Table 3.2 Detailed grain size analysis of suspended river solids and continental shelf sediments from the Waipaoa River catchment.

|  | <b>Waipaoa River</b> | <b>Shelf<br/>4-6 cm</b> | <b>18-19 cm</b> | <b>31-33cm</b> |
|--|----------------------|-------------------------|-----------------|----------------|
| <b>&gt;25 <math>\mu\text{m}</math></b> | 7.89                 | 80.55                   | 5.54            | 81.27          |
| <b>2-25 <math>\mu\text{m}</math></b>   | 86.52                | 17.02                   | 75.64           | 16.43          |
| <b>&lt;2 <math>\mu\text{m}</math></b>  | 5.59                 | 2.43                    | 18.82           | 2.30           |

The river suspension was sampled during period of high discharge. The continental shelf sediment core was chosen to include a sample (18-19 cm) from a Cyclone Bola flood layer.

### 3.2 Clay Mineralogy

A summary of the estimation of clay mineral percentages from XRD results using the Biscaye method (1965) is found in Table 3.3. Minor differences in illite and smectite composition are found between the Whangai mudstone and Tikhore sandstone.

Diffraction patterns for the Tarndale and Whakarau Road ash samples did not produce significant peaks for clay minerals determined in Biscaye’s method, suggesting a dominance of non-crystalline solids. Only a weak illite peak was present in the Tarndale Road ash sample which disappeared upon heating. The Te Karaka samples showed increasing mineral weathering

(2:1-1:1) with increasing depth probably due to soil formation processes. There appears to be substantial differences in the clay mineralogy of the suspended sediments collected from the Waipaoa and Waiapu Rivers, where the Waipaoa contained a higher concentration of smectite and the Waiapu contained a higher concentration of illite. The clay mineralogy of the Waiapu shelf sediments resembles that of the Waiapu suspension.

The Poverty Bay core U2303 at 27 mwd shows some vertical stratification in clay mineralogy. The samples at 18-19 cm and 31-33 cm show mineralogy similar to that measured in the Waipaoa River suspension. The 4-6 cm sample, in contrast, is more like the Waiapu River suspension in that it contains less smectite and substantially greater amounts of illite than do the lower two samples. One possible explanation for these results may indicate transport of Waiapu sediment from the north into Poverty Bay.

Table 3.3 Results of Biscaye's method for quantification of clay minerals by X-ray diffraction (based on the Mg<sup>+2</sup>-ethylene glycolated (liquid) treatment).

| Sample ID                                     | Weighted Smectite Peak (17Å) | Weighted Illite Peak (10Å) | Weighted Kaolinite Peak (7/3.58Å) | Weighted Chlorite Peak (7/3.54Å) | % Smectite | % Illite | % Kaolinite | % Chlorite |
|---|------------------------------|----------------------------|-----------------------------------|----------------------------------|------------|----------|-------------|------------|
| <b>Soils and Ashes</b>                        |                              |                            |                                   |                                  |            |          |             |            |
| Tarndale Road topsoil (10 cm)                 | No peak                      | No peak                    | No peak                           | No peak                          | 0.00       | 0.00     | 0.00        | 0.00       |
| Tarndale Road ash (80 cm)                     | No peak                      | No peak                    | No peak                           | No peak                          | 0.00       | 0.00     | 0.00        | 0.00       |
| Te Karaka topsoil (10 cm)                     | 0.0043                       | 0.0148                     | 0.0076                            | No peak                          | 16         | 55       | 29          | 0.00       |
| Te Karaka ash (13 cm)                         | 0.0164                       | 0.0172                     | No peak                           | No peak                          | 49         | 51       | 0.00        | 0.00       |
| Te Karaka subsoil (43 cm)                     | 0.0339                       | 0.0344                     | 0.0048                            | No peak                          | 47         | 46.5     | 6.5         | 0.00       |
| Whakarau Road ash (near surface)              | No peak                      | No peak                    | No peak                           | No peak                          | 0.00       | 0.00     | 0.00        | 0.00       |
| <b>Rocks</b>                                  |                              |                            |                                   |                                  |            |          |             |            |
| Whangai Fm. Mudstone                          | 0.0326                       | 0.1428                     | 0.0348                            | 0.0348                           | 13         | 59       | 14          | 14         |
| Tikihore Fm. Sandstone                        | 0.0183                       | 0.1408                     | 0.0535                            | 0.0535                           | 7          | 53       | 20          | 20         |
| <b>Suspended River Solids</b>                 |                              |                            |                                   |                                  |            |          |             |            |
| Waipaoa River suspension (4.83 m)             | 0.0303                       | 0.0124                     | 0.0159                            | 0.0159                           | 41         | 17       | 21          | 21         |
| Waiapu River suspension (5.40 m)              | 0.0088                       | 0.1704                     | 0.02873                           | 0.05747                          | 3          | 64       | 11          | 22         |
| <b>Shelf Sediments</b>                        |                              |                            |                                   |                                  |            |          |             |            |
| Waiapu shelf sediment, MC3, 43 mwd (1-2 cm)   | 0.0387                       | 0.0932                     | 0.01287                           | 0.0092                           | 25         | 61       | 8           | 6          |
| Waiapu shelf sediment, MC10, 117 mwd (1-2 cm) | 0.015                        | 0.0304                     | 0.00587                           | 0.01173                          | 24         | 48       | 9           | 19         |
| Poverty Bay Core U2303 (4-6 cm)               | 0.0066                       | 0.0216                     | 0.0027                            | 0.0027                           | 20         | 64       | 8           | 8          |
| Poverty Bay Core U2303 (18-19 cm)             | 0.0061                       | No peak                    | 0.0031                            | 0.0031                           | 38         | 23       | 19.5        | 19.5       |
| Poverty Bay Core U2303 (31-33 cm)             | 0.0086                       | No peak                    | 0.00147                           | 0.00293                          | 48         | 25       | 9           | 18         |

These are semi-quantitative estimates and based on ratios of peak intensity. Percent error  $\pm$  10%.

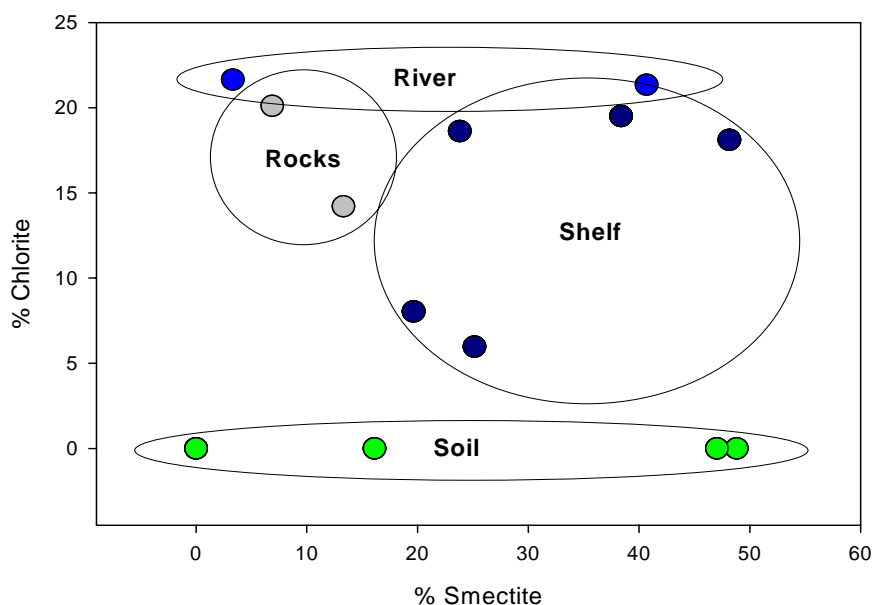


Figure 3.1 Clay compositions of sediment sources (rocks and soil) compared with a short-term sink (the river) and a longer-term sink (the shelf). Chlorite is indicative of bedrock-derived sediment while smectite is dominant in the soils.

### 3.2.1 Rock Mineralogy

The bedrock lithology of the catchments includes a mix of mudstones and sandstones with similar clay mineralogy. The clay sized fraction (<2  $\mu\text{m}$ ) of mudstone (Whangai Fm.) and sandstone (Tikiore Fm.) in the two watersheds is composed of illite, kaolinite, chlorite, and smectite; interstratified illite-smectite was also identified in the mudstone (Figure 3.2). Quartz was clearly identified in all the samples with reflections at 0.425 and 0.331 nm in XRD (Moore and Reynolds, 1997). Quartz was also identified in FTIR spectra of all samples by the doublet at 798 and 779  $\text{cm}^{-1}$  (Figure 3.3) indicating the stretching of Si-O groups within the crystalline structure (Madejová and Komadel, 2001).

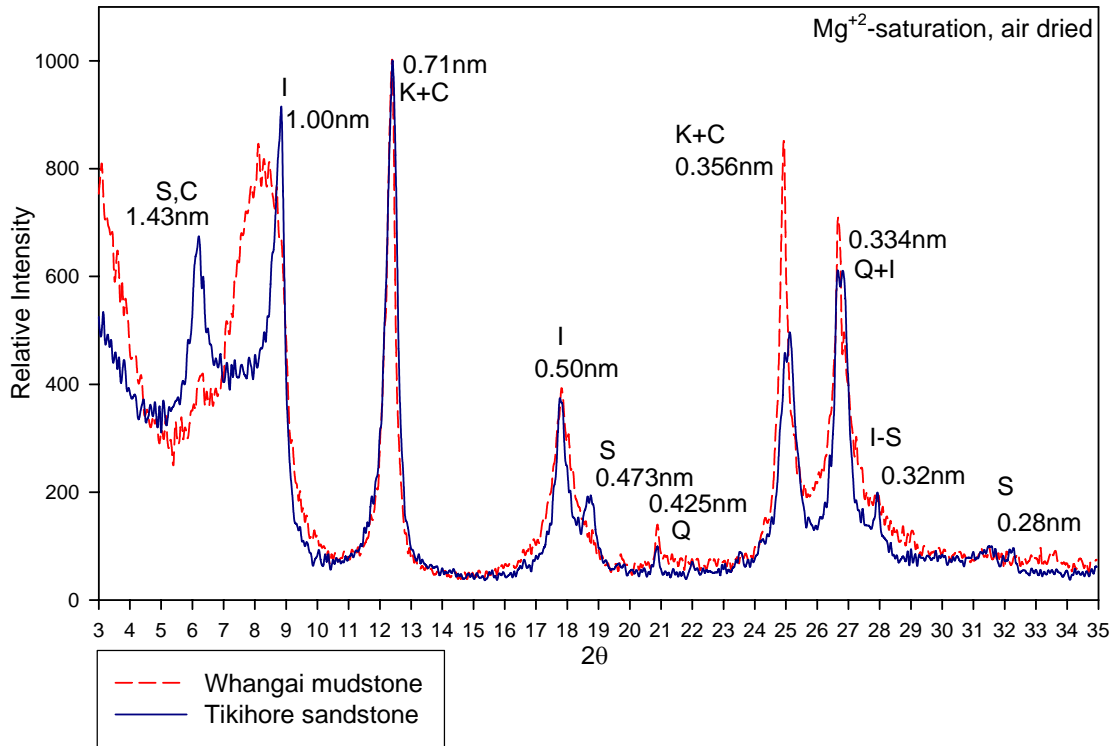


Figure 3.2 XRD patterns of Mg<sup>2+</sup>-saturated, air dried slides for the Whangai and Tikhore Formations. Clays identified include kaolinite (K; 0.71, 0.356 nm), chlorite (C; 1.43, 0.71, 0.356 nm), illite (I; 1.00, 0.50, 0.334 nm), and smectite (S; 1.43, 0.473, 0.32, 0.28 nm). Quartz (Q) was identified by the peaks at 0.425 and 0.334 nm. Mineralogy was confirmed by exposure to ethylene glycol.

XRD analysis revealed that the kaolinite reflections at 0.713 and 0.356 nm were absent when the sample was heated to 550°C; this temperature causes the kaolin structure to decompose differentiating kaolinite from chlorite. The XRD peaks used to identify illite were at 1.00, 0.497 and 0.334 nm. After glycolation, an observed expansion of the smectite layers within a random or regularly interstratified mixed-layer illite-smectite was seen in the mudstone diffractogram pattern confirming the presence of these clays. Expansion of the smectite layers in the interstratified illite-smectite was seen around the peaks for illite and smectite.

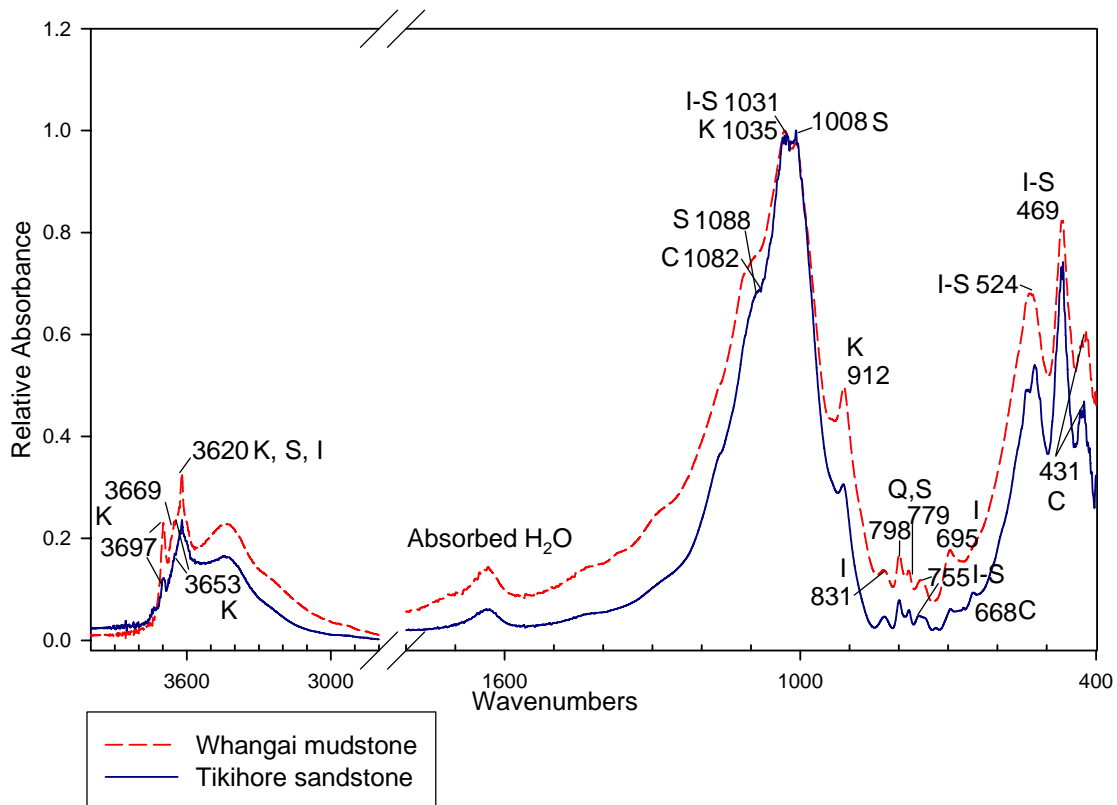


Figure 3.3 FTIR spectra of  $<2\mu\text{m}$  fraction of the source rocks. Clay minerals identified include kaolinite (K; 3697, 3669, 3653, 3620, 1035, 912  $\text{cm}^{-1}$ ), chlorite (C; 1082, 668, 431  $\text{cm}^{-1}$ ), illite (I; 3620, 831, 695  $\text{cm}^{-1}$ ), smectite (S; 3620, 1088, 1008, 779  $\text{cm}^{-1}$ ), and interstratified illite-smectite (I-S; 1031, 755, 524, 469  $\text{cm}^{-1}$ ). Quartz (Q) is identified by the 798, 779  $\text{cm}^{-1}$  doublet.

Figure 3.3 shows two mineral FTIR spectra representative of the variable compositions of these rocks. The Whangai mudstone presented peaks with a higher relative absorbance than the Tikihore sandstone. Stretching of internal OH groups within the kaolinite structure produce the 3697-3620  $\text{cm}^{-1}$  doublet with other diagnostic peaks including 1035 and 912  $\text{cm}^{-1}$ . The presence of the 3653  $\text{cm}^{-1}$  band is a broadening result and replacement of the 3669-3652  $\text{cm}^{-1}$  doublet indicated some disorder within the kaolin structure (Wilson, 1994). Diagnostic peaks for chlorite were observed at 1082, 668 and 431  $\text{cm}^{-1}$ . Illite is present in FTIR with the doublet at 831-695  $\text{cm}^{-1}$  and smectite is identified with the peaks at 1088 and 799  $\text{cm}^{-1}$ . The interstratified illite-smectite component of the mudstone

was more easily observed in FTIR than XRD, with strong peaks present at 1031, 755, 524 and 469  $\text{cm}^{-1}$ . The mineralogy identified in FTIR is consistent with that found by XRD.

### **3.2.2 Soil Mineralogy**

The soil samples displayed weaker signals and produced different patterns in XRD and FTIR than the rocks. The soils contained less crystalline minerals, as indicated by the weak reflections in XRD and the presence of interstratified clay peaks. The  $\text{H}_2\text{O}$  and Si-OH stretching region ( $3700\text{-}3000\text{cm}^{-1}$ ) in FTIR spectra were marked by broad peaks (Figure 3.5). When comparing the FTIR spectra, the  $\text{H}_2\text{O}$  and Si-OH region show a large increase in the stretching of the bonds in this region relative to the rocks. This can be interpreted as the soil clay minerals being more hydrated (containing more absorbed water on the mineral particles) than the rocks, which is probably removed during diagenesis.

The Andic soils consist of a mixed mineralogy derived from the weathering of the volcanic ash and through active transformations in the soil to include kaolinite, smectite, illite and interstratified clays (Buol et al., 2003). Within the watersheds, episodic volcanic eruptions deposit tephra that contribute a unique addition of poorly crystalline minerals (i.e. allophane) to the soils. Soil samples from two localities were collected in the Waipaoa catchment containing two distinct ash layers; a third separate ash layer was also selected for analysis. A synthetic allophane standard was beneficial for the identification of allophane in the ashes and was used to define diagnostic peaks that may be expressed in the ashes when analyzed by FTIR. Samples containing allophane are further discussed in Section 3.2.3 (Ash Mineralogy).

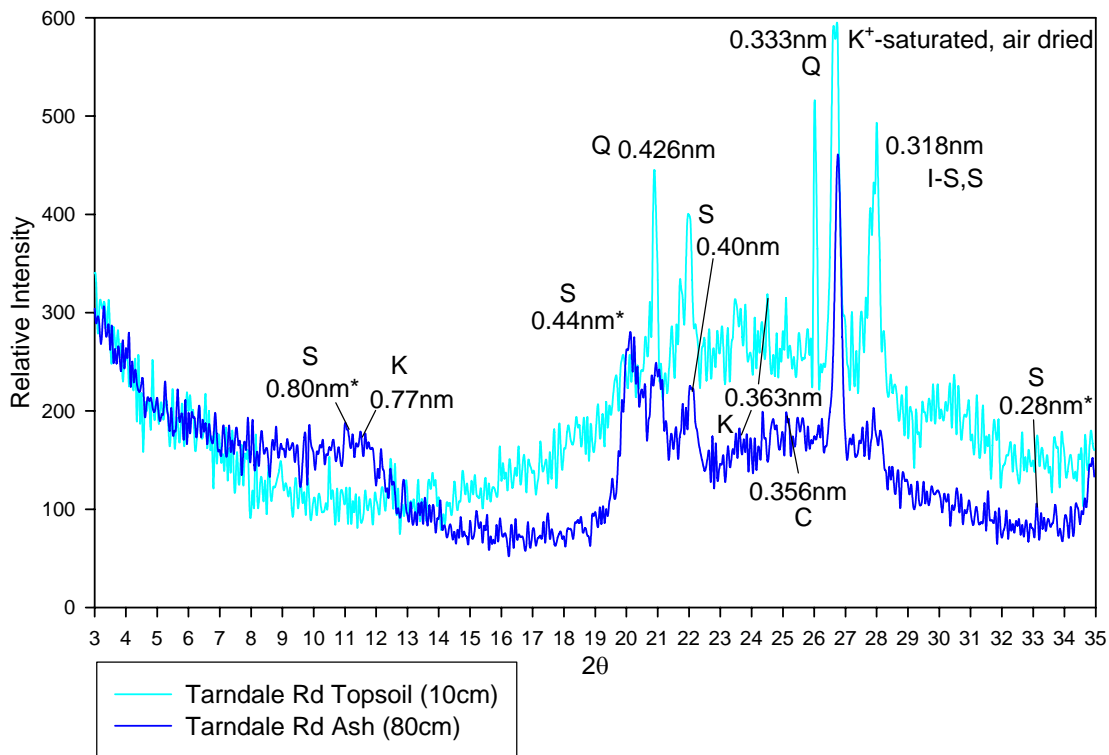


Figure 3.4 XRD pattern for Tarndale Road topsoil and ash layer,  $K^+$ -saturated and air dried, \* refer to peaks identified by  $Mg^{+2}$ -saturation and ethylene glycol treatments. Quartz (Q; 0.426, 0.333 nm) was the only crystalline mineral identified. Clay minerals identified include disordered to weakly structured kaolinite (K; 0.77, 0.363 nm), smectite (0.80, 0.44, 0.40, 0.318, 0.28 nm), and chlorite (0.77, 0.356 nm).

Diffraction patterns for the Tarndale Road topsoil (10 cm) and ash (80 cm) produced no significant peaks for crystalline minerals with the exception of quartz. However, weakly crystalline to disordered phases of kaolinite, chlorite, and smectite were found (Figure 3.4). Heating the  $K^+$ -saturated slides to  $550^{\circ}C$  caused the collapse of the kaolin structure, which differentiated it from chlorite. Glycolation of the  $Mg^{+2}$ -saturated slides caused small expansions throughout the scan range. An unidentified mixed-layer clay was observed in the profile after glycolation, and this component was later identified as smectite from FTIR analysis.

FTIR proved a more useful tool for the characterization of the clay mineralogy for the samples collected from the Tarndale Road locality due to the presence of poorly crystalline minerals. The Tarndale Road topsoil (10 cm) appeared to be less weathered than the ash layer (80 cm) with peaks less sharp with broad shoulders as can be seen in Figure 3.4. The kaolin doublet at 3669-3655  $\text{cm}^{-1}$  is representative of disordered kaolinite in the sample (Wilson, 1994). Kaolin is also denoted by additional peaks at 3619, 1037, 916, 539 and 493  $\text{cm}^{-1}$ . A weak peak with broad shoulders is found at 694  $\text{cm}^{-1}$  and is attributed to illite. The spectrum for the ash layer (80 cm) produced sharper peaks indicative of a higher stage of development. Some weak characteristic chlorite and mixed-layer chlorite-smectite peaks are found at 3567, 1074, 669 and 463  $\text{cm}^{-1}$ . Smectite was identified from the characteristic peaks present at 1087, 1082 and 916  $\text{cm}^{-1}$  in FTIR. In the topsoil, carbonate peaks were present at 1458 and 1411  $\text{cm}^{-1}$ .

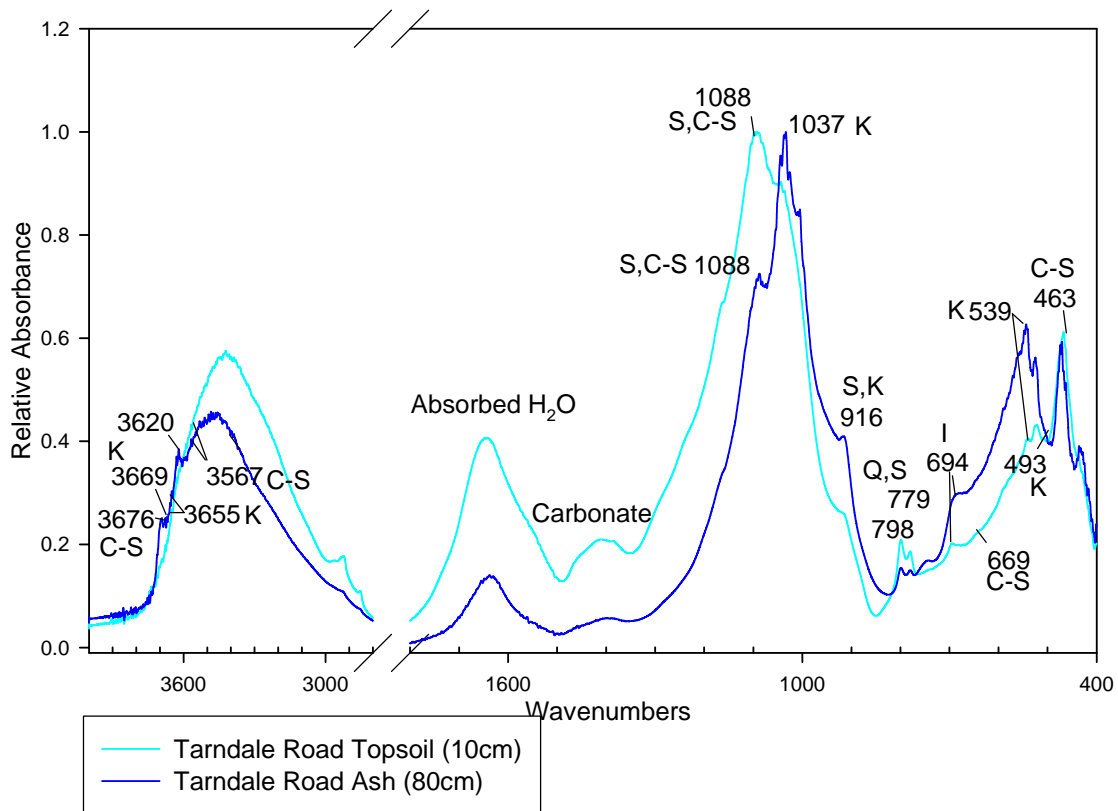


Figure 3.5 FTIR spectra for topsoil and an ash layer at the Tarndale Road locality. Clays identified include kaolinite (K; 3669, 3655, 3620, 1037, 916, 539, 493 cm<sup>-1</sup>), illite (I; 694 cm<sup>-1</sup>), smectite (S; 1088, 916, 798 cm<sup>-1</sup>), and interstratified chlorite-smectite (C-S; 3676, 3567, 1088, 669, 463 cm<sup>-1</sup>). Quartz (Q) was identified by the 798, 779 cm<sup>-1</sup> doublet and carbonate was present with peaks at 1458 and 1411 cm<sup>-1</sup>.

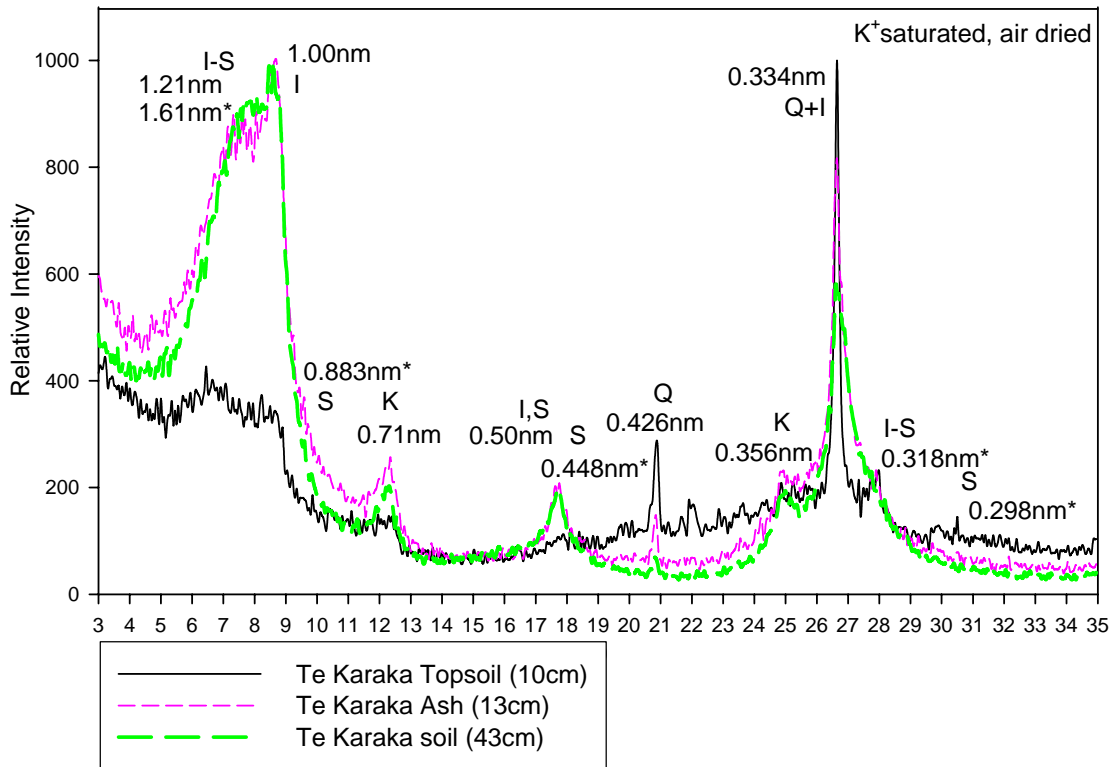


Figure 3.6 XRD patterns for the topsoil and ash layers from the Te Karaka locality, K<sup>+</sup>-saturated, air dried; \* refer to peaks identified by Mg<sup>+2</sup>-saturation and ethylene glycol treatments. Clays identified include kaolinite (K; 0.71, 0.356 nm), illite (I; 1.00, 0.50, 0.334 nm), smectite (S; 1.61, 0.883, 0.448, 0.298nm) and interstratified illite-smectite (I-S; 1.21, 0.50, 0.318nm). Quartz (Q) was also identified with peaks at 0.426 and 0.334 nm.

The horizons sampled from the Te Karaka locality closely resembled each other, with changes to more crystalline clays observable with increasing depth in the profile. Figures 3.6 and 3.7 show that the clays in the profile are composed of kaolinite, smectite, illite and interstratified clay, as identified by both XRD and FTIR. Beginning with the topsoil (10 cm), the degree of development increased with depth due to active transformations in the soil. Low relative intensities of kaolinite stood out in all the treatments for XRD. The absence of the 0.354 nm peak in the XRD pattern (Figure 3.6) may be a signal of disorder in the kaolin structure (Moore and Reynolds, 1997). Illite reflections were strongly present in the K<sup>+</sup>-

saturated air-dried slide, but decreased in relative intensity to being nearly undetectable upon heating the sample. XRD results indicated the presence of smectite in the topsoil (10 cm) and ash layers (13 cm) with peaks at 1.61, 1.43, 0.719, 0.483, 0.355 and 0.298 nm that expanded when exposed to liquid ethylene glycol. Smectite was the dominant mineral at the 43 cm horizon, with lesser amounts of illite and disordered kaolinite. The smectite reflections clearly stand out after glycolation, where the 1.61 nm peak shifted to 1.89 nm; a decrease in relative intensity was also observed (Appendix). Although XRD does confirm the presence of crystalline clays in the ash layer (13 cm), XRD does not provide any evidence to confirm the presence of allophane in the ash layer (13cm).

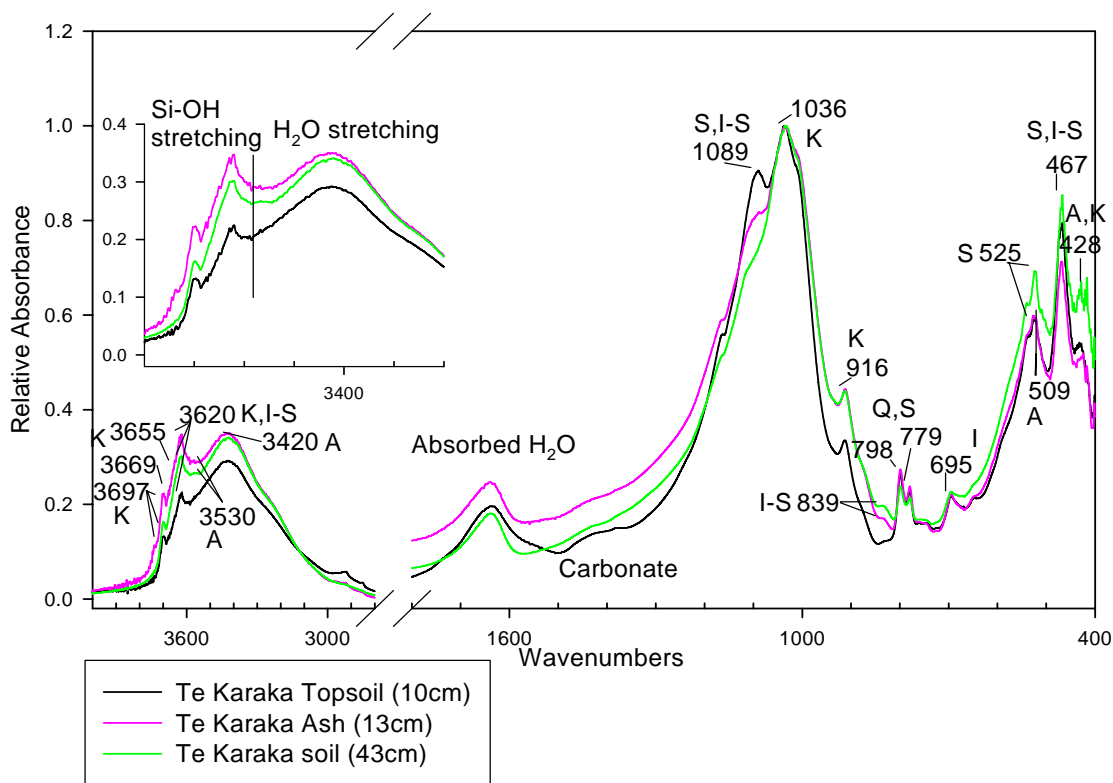


Figure 3.7 FTIR spectra for the topsoil and ash layers at the Te Karaka site. Clay and short range-order minerals identified include kaolinite (K; 3697, 3669, 3655, 3620, 1036, 916, 428  $\text{cm}^{-1}$ ), smectite (S; 1089, 839, 798, 525, 467  $\text{cm}^{-1}$ ), interlayered illite-smectite (I-S; 3620, 1089, 839, 467  $\text{cm}^{-1}$ ), and allophane (A; 3530, 3420, 509, 428  $\text{cm}^{-1}$ ). Quartz (Q) was identified by the 798, 779  $\text{cm}^{-1}$  doublet. Carbonate (1428, 1459  $\text{cm}^{-1}$ ) was present in the

topsoil. The inset shows increasing hydration within the stretching regions of internal Si-OH and H<sub>2</sub>O in the range of 3800-3200 cm<sup>-1</sup>.

Kaolinite was identified in the FTIR spectrum by the 3697-3620 cm<sup>-1</sup> doublet and the peak at 1036 cm<sup>-1</sup>. However, shifts of the 916 cm<sup>-1</sup> to 912 cm<sup>-1</sup> and 3669-3655 cm<sup>-1</sup> absorption bands identify disorder in the kaolin structure with internal OH groups bending and stretching (Farmer and Russell, 1966). Smectite was identified with absorption bands at 1089, 524 and 467 cm<sup>-1</sup>. The Te Karaka profile showed a flattening of the 1089 cm<sup>-1</sup> peak with progression downward in the profile. This is interpreted to reflect the transformation of volcanic glass and short range-order minerals into transitional or more stable clays.

Additionally, the broadening of the Si-OH and H<sub>2</sub>O stretching regions is the result of surface hydration and suggests the presence of allophane in the ash sample (Wilson, 1994). The ash layer at 13 cm depth contained some disordered kaolin, illite, smectite and interstratified illite-smectite from FTIR analysis. The relatively broad peaks identified a transitional illite-smectite component with low absorbance over the entire scan range. These absorption bands occur at 3621, 1088, 839, 695, 525 and 468 cm<sup>-1</sup> with some overlap of the smectite and illite peaks. Carbonate was identified in the topsoil with diagnostic peaks at 1459 and 1428 cm<sup>-1</sup>. The broadening of unresolved OH-stretching bands at 3420, 509 and 428 cm<sup>-1</sup> is typical of allophane (Wilson, 1994). The ash layer had a greater relative absorbance than the other two horizons in the Si-OH and H<sub>2</sub>O stretching regions and can be interpreted as the presence of allophane (Wilson, 1994).

### **3.2.3 Ash mineralogy**

Poorly crystalline minerals are not easily characterized by XRD (Farmer et al., 1977; Parfitt, 1990; Ohashi et al., 2002; Basile-Doelsch et al., 2005). Figures 3.7 and 3.8 show a

comparison of XRD and FTIR results of three distinct ash layers within the Waipaoa catchment. It is expected that the ash layers would contain a higher concentration of poorly crystalline minerals (i.e. allophane) that produce broad absorbance bands.

Significant diffraction peaks were not present in XRD patterns of the three ash samples; rather, the patterns exhibited broad maxima across different regions that suggest the presence of non-crystalline and short-range order minerals. However, allophane could not be clearly identified in the diffractograms from the soil samples due to its poorly crystalline structure. Quartz was the only noteworthy (non-clay) mineral detected by XRD in the ash samples (Figure 3.8). Table 3.3 provides initial clay mineral estimations for all the ash layers, but upon heating the slides, kaolinite, illite, and montmorillonite peaks disappeared, thus leaving the initial estimations according to Biscaye not consistent. The Te Karaka ash did show the presence of illite, smectite, and disordered kaolinite while the Tarndale Road ash appeared to contain disordered kaolinite and smectite. As can be seen in Figure 3.8, the only changes noticed with the heating and glycolation treatments (Appendix) were decreases in relative intensity.

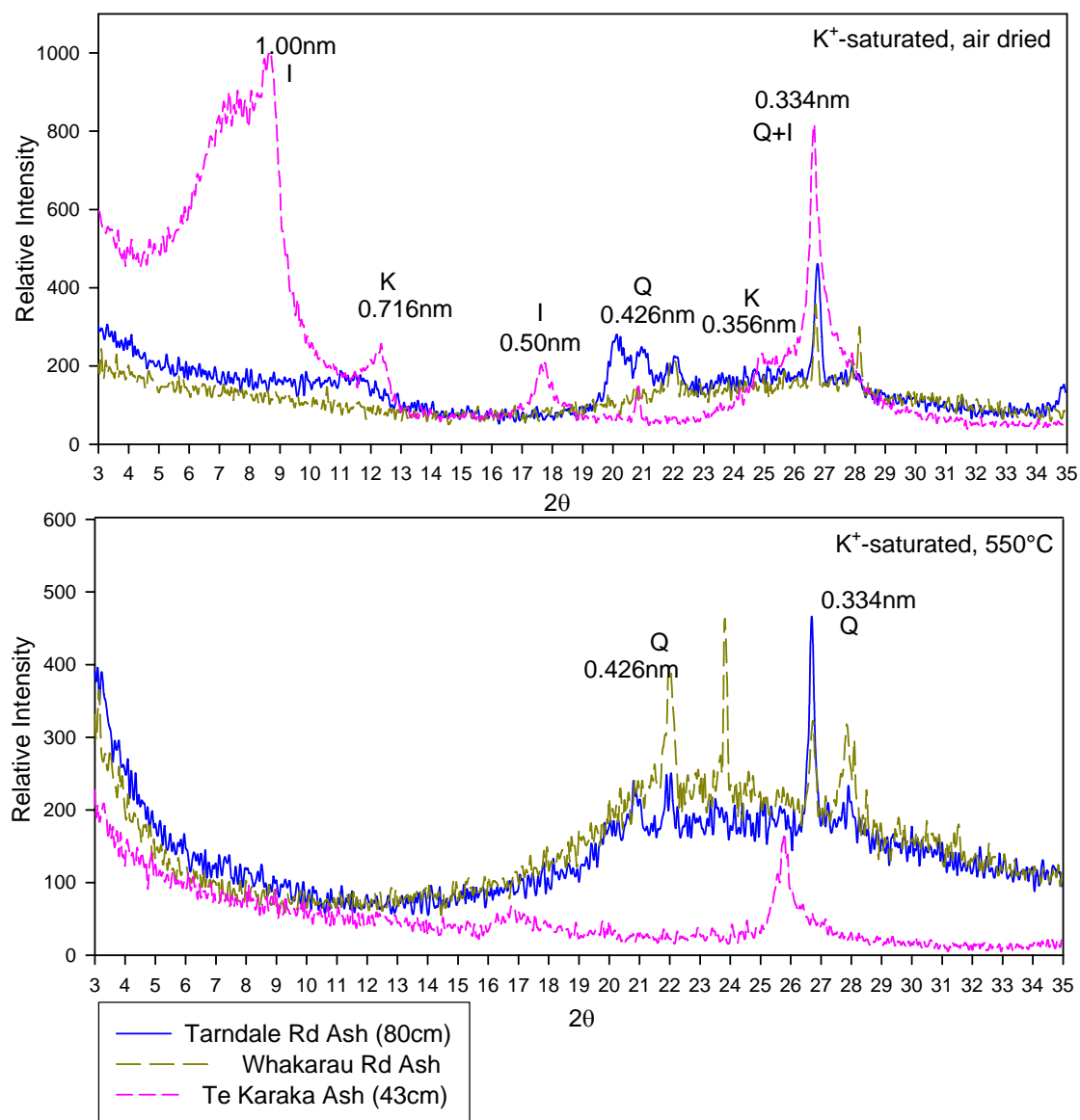


Figure 3.8 XRD results of the three ash layers (Tarndale and Whakarau Roads, Te Karaka). Top: K<sup>+</sup>-saturated, air dried. Bottom: K<sup>+</sup>-saturated, 550°C. Minerals identified include kaolinite (K; 0.716, 0.356 nm), illite (I; 1.00, 0.50, 0.334 nm), and quartz (Q; 0.426, 0.334 nm).

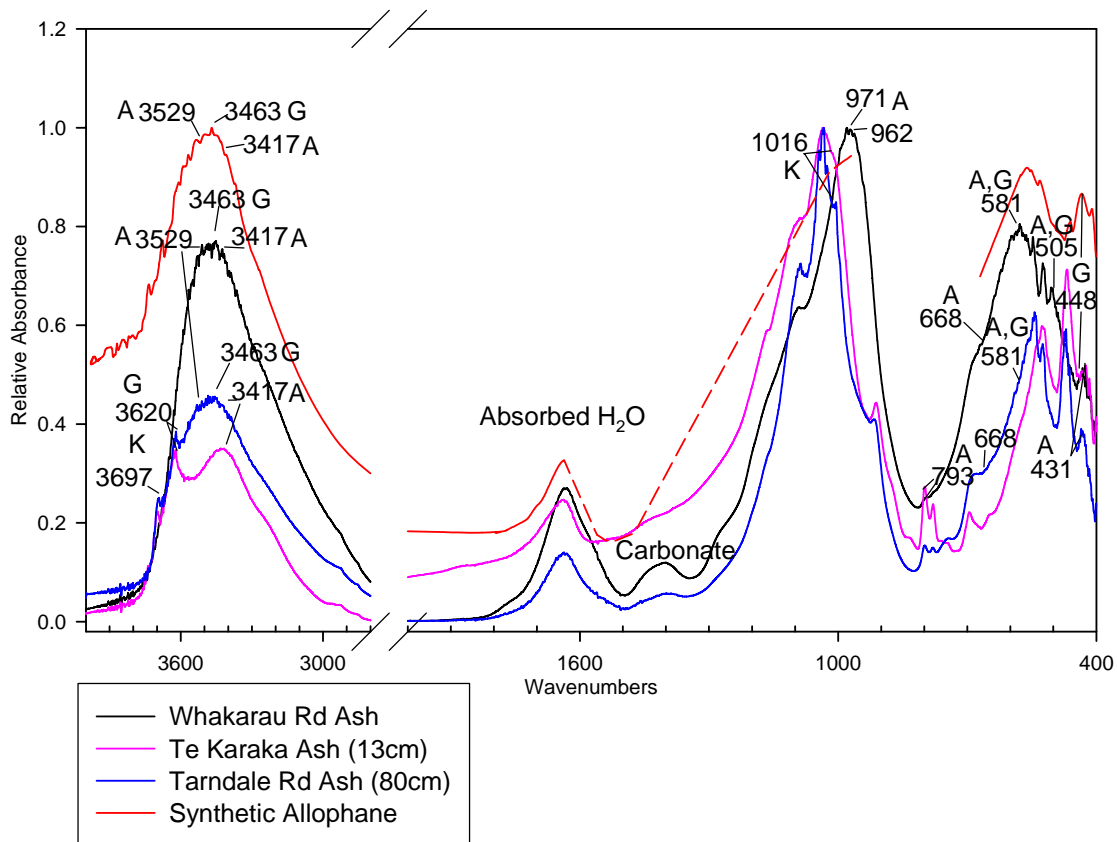


Figure 3.9 FTIR spectra of ash layers and synthetic allophane. Short range-order minerals identified include allophane (A; 3529, 3417, 971, 962, 793, 668, 581, 505, 431  $\text{cm}^{-1}$ ), gibbsite (G; 3620, 3463, 581, 505, 448  $\text{cm}^{-1}$ ), kaolinite (K; 3697, 3620, 1016  $\text{cm}^{-1}$ ). Carbonate (1459, 1420  $\text{cm}^{-1}$ ) was found in the Whakarau and Tarndale Rd ashes. Increasing hydration indicated the presence of allophane. \*Allophane standard line is dashed where inferred.

For FTIR, the Whakarau Road ash layer displayed broad peaks in the entire scan range (as seen in Figure 3.9). Diagnostic peaks for crystalline minerals were difficult to distinguish within the fingerprint region. This ash exhibited Al-Si-O deformation (or bending) occurring in the range of 540-520  $\text{cm}^{-1}$  (Madejová and Komadel, 2001). Peaks characteristic of allophane were found to be the most prevalent in this ash compared to the ashes sampled at the Tarndale Road and Te Karaka sites. Major peaks within the fingerprint region indicative of allophane were found at 3529, 3417, 971, 962, 668, 597, 505 and 431

$\text{cm}^{-1}$ . The 971-962  $\text{cm}^{-1}$  doublet had the highest relative absorbance of 0.997 and 0.988, respectively. Also observed in this layer was gibbsite with absorbance bands at 3463, 581, 559, 502 and 448  $\text{cm}^{-1}$ . Carbonate was also present in the Whakarau and Tarndale Road ash layers with peaks identified at 1459 and 1420  $\text{cm}^{-1}$ .

Stretching of absorbed water found within the internal solid structure produces the characteristic wide absorption bands found in the range of 3600-3300  $\text{cm}^{-1}$ . The Whakarau Road ash layer exhibits the highest peak intensities in this region. The synthetic allophane provided a very distinct spectrum within this range that was useful in positively identifying diagnostic peaks within the 3600-3300  $\text{cm}^{-1}$  region for the ash samples.

### **3.2.4 River Mineralogy**

The river suspensions were collected at a time of high discharge when it was suspected that material was well mixed with respect to particle size and serves as a representative sample of material being deposited on the adjacent shelf. The mineralogy of the suspensions reflects the mixed mineralogy of sediment being derived from the erosion of the volcanic soils and the gully erosion of the rocks. Clay minerals identified in the Waipaoa and Waiapu Rivers included smectite, illite, chlorite, kaolin, and an interstratified illite-smectite. Kaolinite peaks at 0.71 and 0.353 nm are distinguished from chlorite when the slides are heated to 550°C, which causes the decomposition of the kaolin structure (Figure 3.10). It was observed in XRD that the chlorite peaks decreased in relative intensity when heated. The Waipaoa River suspension contained a substantially higher concentration of smectite than the Waiapu (Table 3.3). After glycolation, shifts in peak position and decreases in relative intensity are seen within the smectite from the Waiapu River suspension. Smectite and illite had peaks disparate from transitional illite-smectite clays. The smectite component

of the interstratified illite-smectite also expands after glycolation. FTIR was consistent with the clay mineralogy determined by XRD.

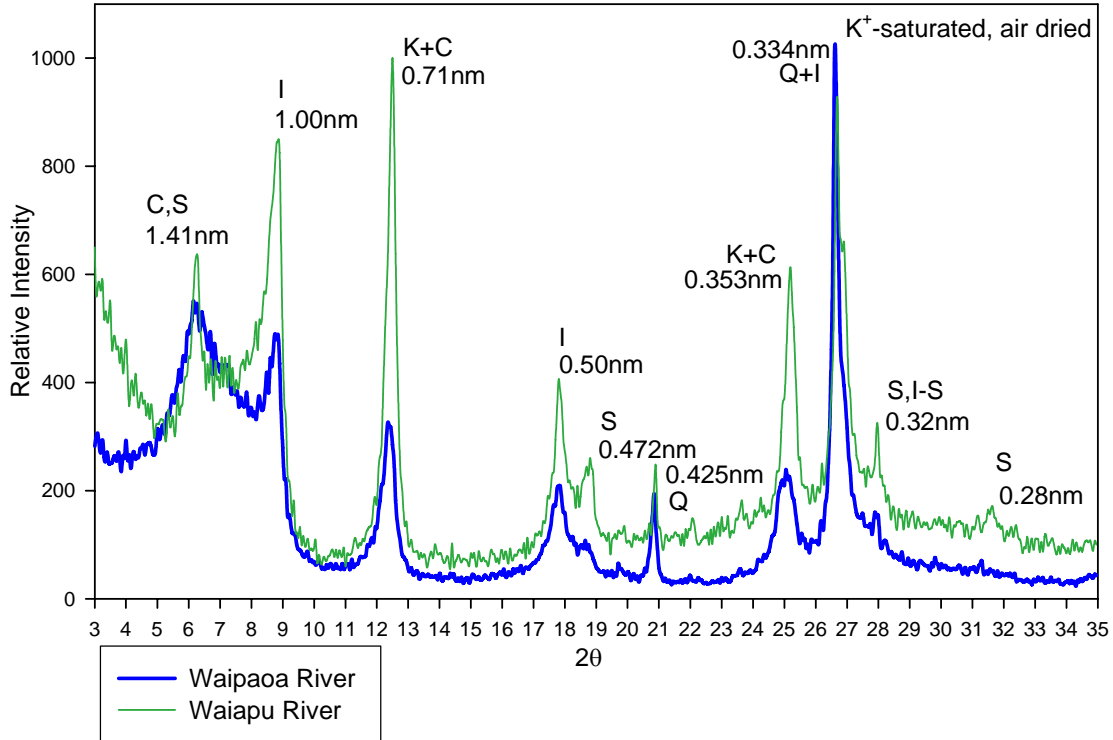


Figure 3.10 XRD of Waipaoa and Waiapu river suspensions,  $K^+$ -saturated, air dried. Clays identified include kaolinite (K; 0.71, 0.353 nm), illite (I; 1.00, 0.50, 0.334 nm), smectite (S; 1.41, .472, 0.32, 0.28 nm), chlorite (C; 1.41, 0.71, 0.353 nm). Quartz (Q) is identified by peaks at 0.425 and 0.334nm.

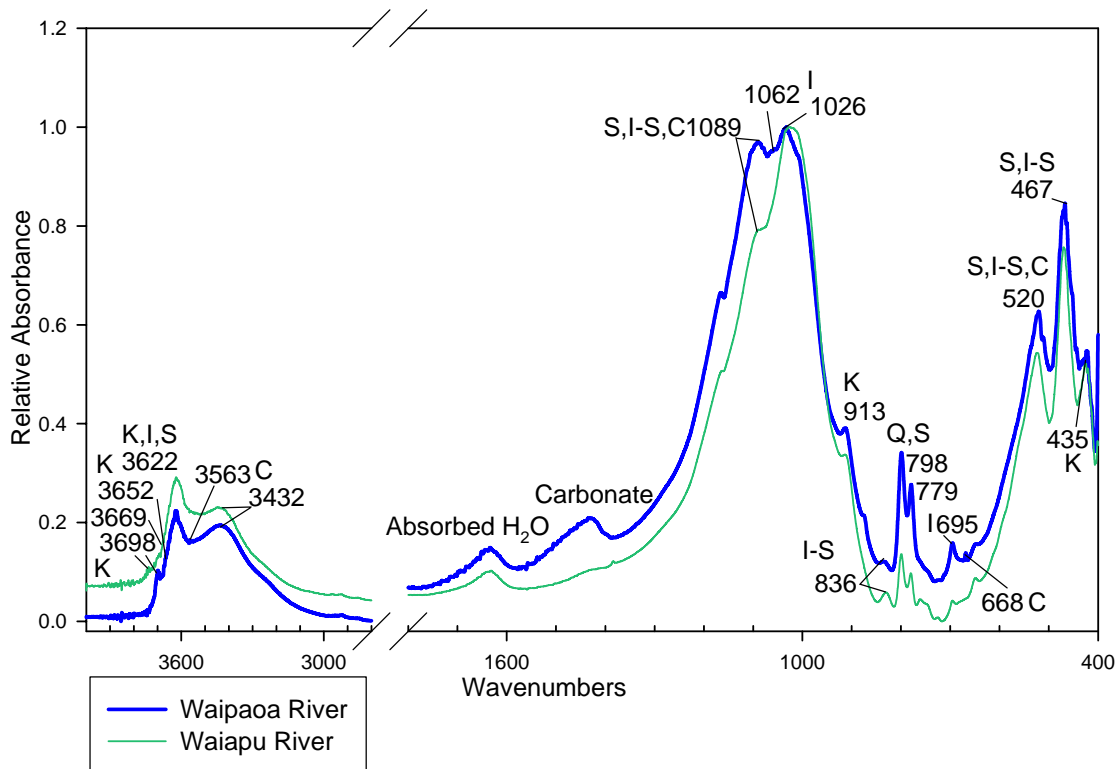


Figure 3.11 FTIR spectra of Waipaoa and Waiapu River suspensions. Clay minerals identified include kaolinite (K; 3698, 3669, 3652, 3620, 913, 435  $\text{cm}^{-1}$ ), illite (I; 3622, 1062, 1026, 831, 695  $\text{cm}^{-1}$ ), smectite (S; 3622, 1089, 798, 520, 467  $\text{cm}^{-1}$ ), chlorite (C; 3563, 3432, 1098, 668, 520  $\text{cm}^{-1}$ ), interstratified illite-smectite (I-S; 3622, 1089, 836, 520, 467  $\text{cm}^{-1}$ ). Quartz (Q) was identified by the 798-779  $\text{cm}^{-1}$  doublet. Carbonate was identified by the 1469, 1458, 1428  $\text{cm}^{-1}$  peaks.

XRD analysis determined that illite and smectite were the dominant minerals in the Waiapu and Waipaoa suspensions, respectively. Diagnostic FTIR smectite peaks were more prevalent in the spectrum from the Waipaoa based on the presence of the peaks at 3622, 1089, 798, 520 and 467  $\text{cm}^{-1}$  (Figure 3.11). The 3698-3622  $\text{cm}^{-1}$  and 913-435  $\text{cm}^{-1}$  doublets characterized kaolinite. The peaks at 3563, 3432, 668 and 520  $\text{cm}^{-1}$  identified chlorite. Carbonate was present only in the suspended sediment from the Waipaoa River by the peaks at 1469, 1458, and 1428  $\text{cm}^{-1}$ . The Waiapu River suspension showed a lower relative absorbance over the entire scan range when compared to the Waipaoa River suspension.

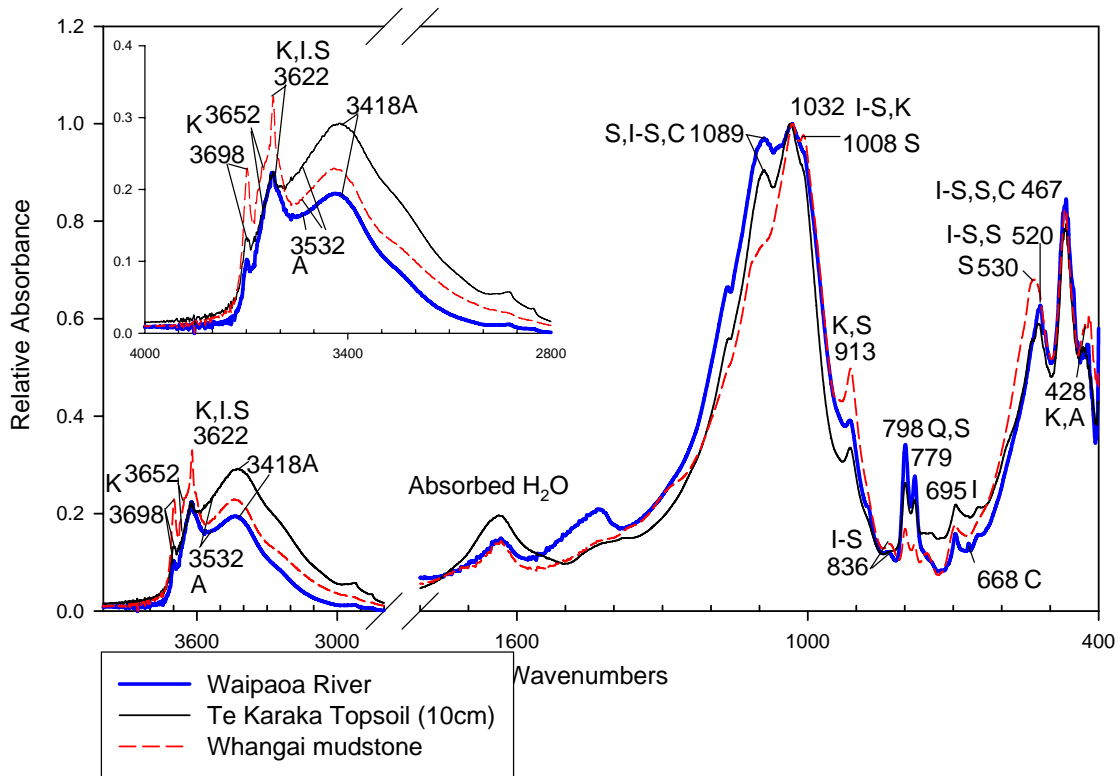


Figure 3.12 FTIR spectral comparisons of Waipaoa River to soil and bedrock samples within the catchment. Clays identified include kaolinite (K; 3698, 3652, 3620, 1032, 913, 428  $\text{cm}^{-1}$ ), illite (I; 3622, 831, 695  $\text{cm}^{-1}$ ), smectite (S; 3622, 1089, 1008, 913, 798, 530, 520, 467  $\text{cm}^{-1}$ ), chlorite (C; 1098, 668, 467  $\text{cm}^{-1}$ ), interstratified illite-smectite (I-S; 1089, 1032, 836, 520, 467  $\text{cm}^{-1}$ ), and allophane (A; 3532, 3418, 428  $\text{cm}^{-1}$ ). Quartz was characterized by the 798-779  $\text{cm}^{-1}$  doublet. The inset shows the 4000-2800  $\text{cm}^{-1}$  range ( $\text{H}_2\text{O}$  and Si-OH stretching) based on kaolinite peaks, marking similarities between the river and soil.

As shown in Figure 3.12, the Waipaoa River produces a spectrum in FTIR that shared many traits common to the bedrock and volcanic soils in the catchment. At the low scan range of 1100-400  $\text{cm}^{-1}$ , the suspended river solids more closely resembles the Whangai mudstone with sharp peaks, but the high end ranging from 4000-2800  $\text{cm}^{-1}$  resemble the topsoil with more absorbed water and greater Si-OH and  $\text{H}_2\text{O}$  stretching than the rocks. The increase in absorbed water may be either a signature of mineral weathering or exposure in the fluvial environment. Apparent contributions from the soil are indicated by the presence of

carbonate in the river suspension which is also seen in the Tarndale Road and Te Karaka topsoil. This provides evidence for the mixing of the distinct sources being transported as suspended sediment in the river, and possibly points to material being derived from not only bedrock but the erosion of soils.

### **3.2.5 Shelf Mineralogy**

Material eroded from catchments is transported by the rivers and eventually deposited on the continental margin. As suspected, clay mineralogy of the samples on the continental margins adjacent to the Waipaoa and Waiapu Rivers bear signatures resembling material from the river suspensions based on XRD and FTIR (Figures 3.13 and 3.14). The spectra indicate the mixed composition of the rocks and soils being derived from gully erosion and landslides within the catchments. For example, FTIR shows the mineral particles in the shelf sediments (Figure 3.14) having more absorbed water. The absorbed water content may be explained by the clay mineral residence in the seabed. The evidence of landslides that occurred in the Waipaoa catchment during Cyclone Bola are one such example of a flood layer preserved in shelf sediment that especially bears a resemblance to the terrestrial soils being eroded.

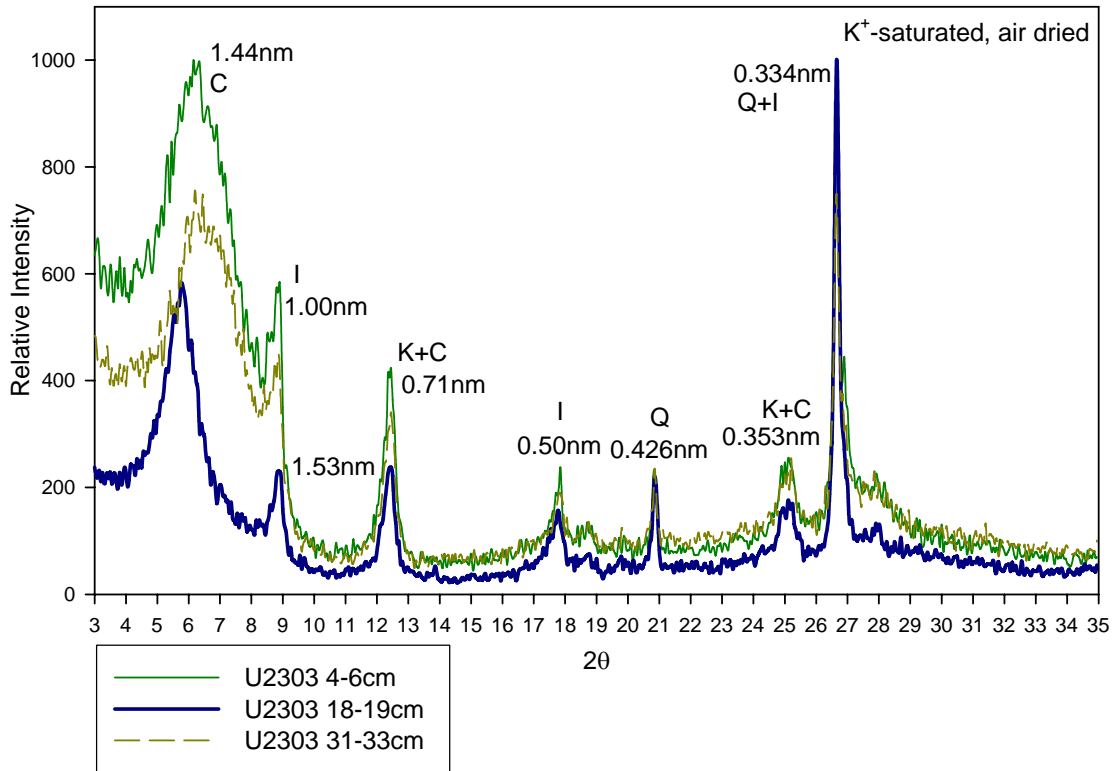


Figure 3.13 XRD results for Poverty Bay (Core U2303) continental shelf sediments off the Waipaoa River. Clays identified include kaolinite (K; 0.71, 0.353 nm), illite (I; 1.00, 0.50, 0.334 nm), and chlorite (C; 1.44, 0.71, 0.353 nm). Quartz (Q) was identified by peaks at 0.426 and 0.334 nm.

The downcore sampling on the Poverty Bay Core U2303 (30 m water depth) resulted in nearly identical spectra in XRD and FTIR with slight variations arising from peak intensities. The 4-6 cm interval exhibited the highest concentration of illite and the lowest concentration of kaolinite and chlorite based on Biscaye's method (1965), but the mineral concentrations changed with progression downcore. Smectite reflections decreased in relative intensity as the slides were heated and exposed to liquid ethylene glycol but the mineral composition increased downcore. Confirmation of the clay mineralogy was based on the heating and glycolation treatments and by FTIR.

The clay mineralogy of the three sampled intervals of the core revealed in FTIR is consistent with what was identified in XRD. In FTIR, the doublets at 3696-3620  $\text{cm}^{-1}$  and 3669-3656  $\text{cm}^{-1}$  along with peaks at 1035, 913 and 413  $\text{cm}^{-1}$  help identify kaolinite. The peaks identifying illite are 3620, 695, 527 and 467  $\text{cm}^{-1}$ ; chlorite was found to be present by the peaks of 1087, 1077, 668 and 463  $\text{cm}^{-1}$ . The diagnostic smectite peaks were observed at 3620, 1087, 1035, 467 and 431  $\text{cm}^{-1}$ . Carbonate was identified by the peaks at 1474, 1458, 1443, and 1430  $\text{cm}^{-1}$  which could be indicative of the addition of marine carbonate.

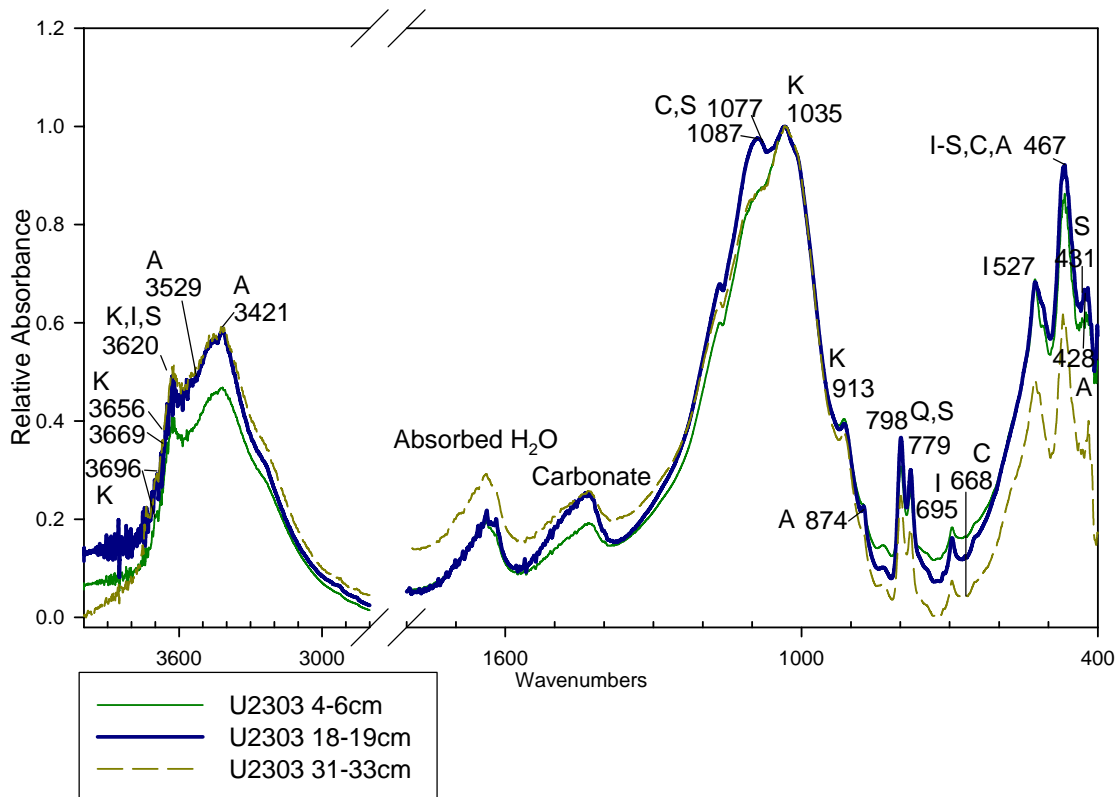


Figure 3.14 FTIR spectra for sediments taken from Core U2303, Poverty Bay, off the Waipaoa River. Clays identified include kaolinite (K; 3696, 3669, 3656, 3620, 1035, 913  $\text{cm}^{-1}$ ), illite (I; 3620, 695, 527  $\text{cm}^{-1}$ ), smectite (S; 3620, 1087, 798, 467, 431  $\text{cm}^{-1}$ ), chlorite (C; 1087, 1077, 668, 467  $\text{cm}^{-1}$ ), and allophane (A; 3529, 3421, 874, 467, 428  $\text{cm}^{-1}$ ). Quartz (Q) is identified by the 798-779  $\text{cm}^{-1}$  doublet. Carbonate is present with peaks at 1474, 1458, 1443, and 1430  $\text{cm}^{-1}$ .

The study of a flood layer (18-19 cm) marked by the higher percentage of fine-grained material (silt and clay, 95%) revealed interesting results based on the mineralogical analysis. In XRD, subtle variations were observed between 19-26° 2θ for the Mg<sup>2+</sup>-glycol treatment where in this range, the flood layer resembled patterns produced by the ash samples. For the ash samples, minor expansions were noted. However, FTIR reveals the presence of allophane in the flood layer based on the presence of signature peaks at 3529, 3421, 874, 469 and 427 cm<sup>-1</sup>. These peaks were not found in the samples above and below the flood layer. The sample from the flood layer (18-19 cm) resembled the spectra of the other sediments in this core closely but with a notable difference in the range of 1200-1000 cm<sup>-1</sup>. This area was broader and had a higher relative absorbance than the other samples.

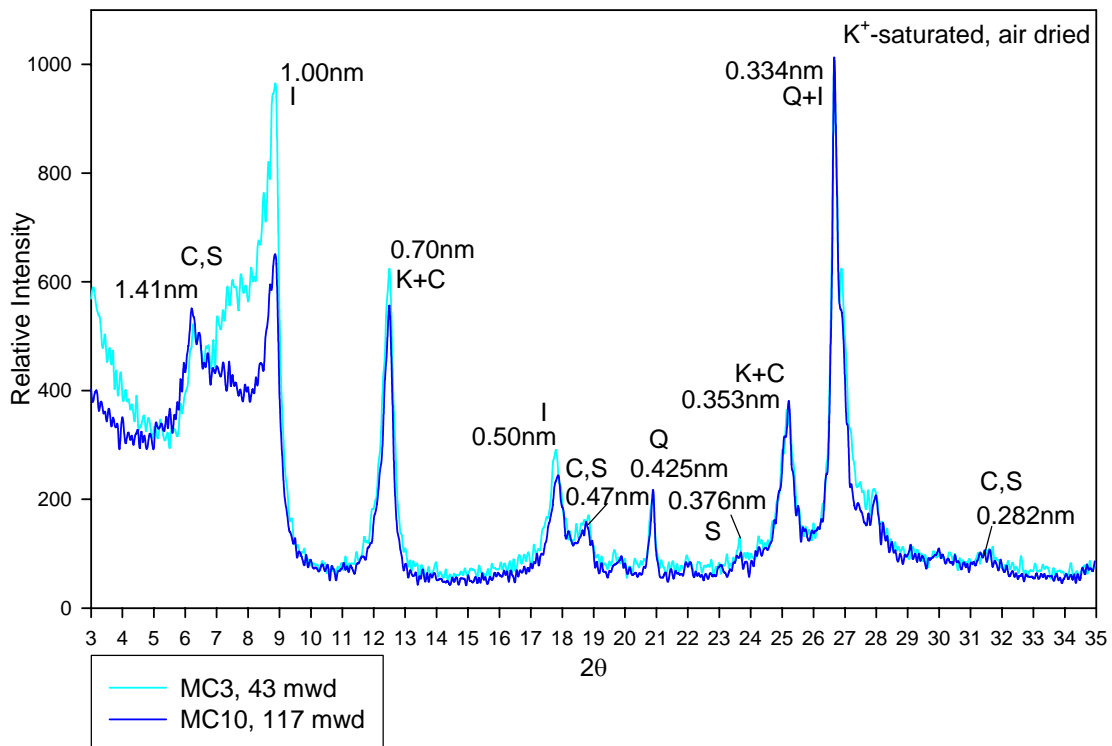


Figure 3.15 XRD results of sediments taken from cores offshore to the Waiapu River, K<sup>+</sup>-saturation, air dried. Clays identified include kaolinite (K; 0.70, 0.353 nm), illite (I; 1.00, 0.50, 0.334 nm), smectite (S; 1.41, 0.47, 0.376, 0.282 nm) and chlorite (C; 1.41, 0.70, 0.353 nm). Quartz (Q) was identified by peaks at 0.425 and 0.334 nm.

Figures 3.15 and 3.16 show XRD patterns and FTIR spectra of continental shelf sediment sampled from 1-2 cm deep in cores MC3 and MC10 taken off the Waiapu River at 43 and 117 m water depth (mwd), respectively. Sediments from these two cores show significant differences in chlorite and illite content based on Biscaye's method, but produced similar patterns in XRD and FTIR. These sediments were dominated by illite and smectite with lesser amounts of chlorite and kaolinite. Upon heating the slides, chlorite concentrations increased in the distal shelf (117 mwd) while illite decreased (Appendix). Sediment taken from the core at 43 mwd produced the opposite results. Figure 3.15 shows the diffractogram patterns for these samples. Peaks used for the identification of kaolinite were located at 0.70 and 0.353 nm. Chlorite was identified by the peaks at 1.41, 0.70, 0.47, 0.353 and 0.282 nm. Illite had characteristic peaks of 1.00, 0.50 and 0.334 nm, while smectite peaks at 1.41, 0.47, 0.376 and 0.282 nm expanded upon glycolation. Additional treatments confirmed the clay mineralogy.

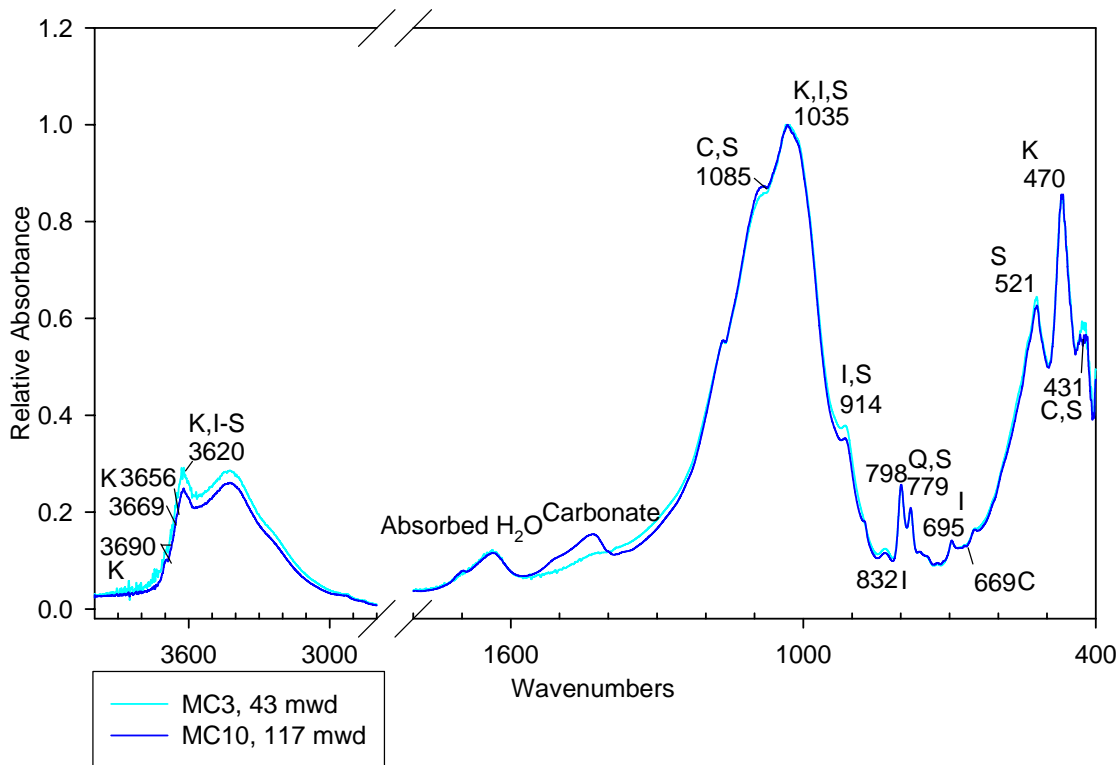


Figure 3.16 FTIR results of continental shelf sediments adjacent to the Waiapu River. Clays identified include kaolinite (K; 3690, 3669, 3656, 3620, 1035, 470  $\text{cm}^{-1}$ ), illite (I; 3620, 1035, 914, 832, 695  $\text{cm}^{-1}$ ), smectite (S; 3620, 1085, 1035, 914, 798, 521, 431  $\text{cm}^{-1}$ ), and chlorite (C; 1085, 669, 431  $\text{cm}^{-1}$ ). Quartz (Q) is identified by the 798-779  $\text{cm}^{-1}$  doublet. Carbonate is present with peaks at 1458, 1431, and 1424  $\text{cm}^{-1}$ .

As with XRD, FTIR spectra showed no major differences in the patterns produced by the  $<2 \mu\text{m}$  fraction at the two shelf sites of the Waiapu are consistent with the clays identified by XRD. As shown in Figure 3.16, the 3690-3620 and 3669-3656  $\text{cm}^{-1}$  doublets and additional peaks 1035 and 470  $\text{cm}^{-1}$  are distinctive of kaolinite. The peaks associated with chlorite are at 1081, 669 and 431  $\text{cm}^{-1}$ . Illite was identified by its distinctive peaks of 1034, 918, 832 and 695  $\text{cm}^{-1}$ . The diagnostic smectite peaks were at 1085, 914 and 521  $\text{cm}^{-1}$ . Carbonate peaks were present at 1458, 1431, and 1424  $\text{cm}^{-1}$ . The stronger signature of carbonate at 117 mwd could indicate that more marine carbonate has been incorporated into

the sediment. Minor variations in relative absorbance were the only differences between the sediment from MC3 and MC10.

### **3.3 Selective Dissolution Studies**

Results of acid ammonium oxalate dissolution for the sample suite are shown in Table 3.4. The Tarndale soil forming on volcanic tephra (Tarndale Road Ash) can first be classified as having andic properties, because  $Al_0 + \frac{1}{2}Fe_0 \geq 2\%$  (Soil Survey Staff, 1999). Other distinctive properties of these soils include a high %OC concentration and dark colors that are strongly exhibited in the topsoil.

As noted in Table 3.4, the Whakarau and Tarndale Road ash layers contained the highest concentration of oxalate extractable Al and Si. The concentrations of Al are slightly lower and Si slightly higher in the Te Karaka topsoil (10 cm) as compared to the subsoil (43 cm deep). The weathering of the volcanic glass and the thickness of the tephra bed would yield the higher concentrations of dissolvable Al and Si as seen in these profiles. The Tarndale and Whakarau Road ash layers contained the highest concentration of extractable Al, which can be attributed to the presence of allophane (as identified in FTIR, Figure 3.8). The values of Al:Si for the ash layers are in the ranges discussed by Parfitt and Henmi (1982), Lowe (1986), Parfitt (1990) and García-Rodeja et al. (2004), indicating allophane in these layers.

Table 3.4 Results of acid ammonium oxalate dissolution of clay samples.

| Sample                        | %Al  | %Fe  | %Si  | Al:Si | %OC*   |
|-------------------------------|------|------|------|-------|--------|
| <b>Soils and Ashes</b>        |      |      |      |       |        |
| Te Karaka topsoil (10cm)      | 0.30 | 0.36 | 0.02 | 12.46 | 5.991  |
| Te Karaka ash (13cm)          | 0.14 | 0.12 | 0.02 | 8.56  | 1.333  |
| Te Karaka subsoil (43cm)      | 0.14 | 0.18 | 0.02 | 6.02  | 0.489  |
| Tarndale Road topsoil (10cm)  | 0.83 | 0.42 | 0.29 | 2.91  | 13.9   |
| Tarndale Road ash (80cm)      | 4.86 | 0.53 | 1.86 | 2.62  | 2.342  |
| Whakarau Road ash             | 4.59 | 0.43 | 2.13 | 2.16  | 2.979  |
| <b>Suspended River Solids</b> |      |      |      |       |        |
| Waipaoa River                 | 0.10 | 0.28 | 0.05 | 1.99  | 0.705  |
| Waiapu River                  | 0.10 | 0.28 | 0.05 | 2.01  | 0.6273 |
| <b>Shelf Sediments</b>        |      |      |      |       |        |
| Waiapu shelf, MC-3, 43 mwd    | 0.12 | 0.50 | 0.04 | 2.88  | 0.7136 |
| Waiapu shelf Mc-10, 117 mwd   | 0.10 | 0.49 | 0.04 | 2.30  | 0.894  |
| Core U2303 4-6 cm             | 0.12 | 0.51 | 0.05 | 2.55  | 0.6139 |
| Core U2303 18-19 cm           | 0.10 | 0.52 | 0.04 | 2.33  | 0.6927 |
| Core U2303 31-33 cm           | 0.12 | 0.56 | 0.05 | 2.59  | 0.5419 |

\*%OC collected by EA during separate analysis.

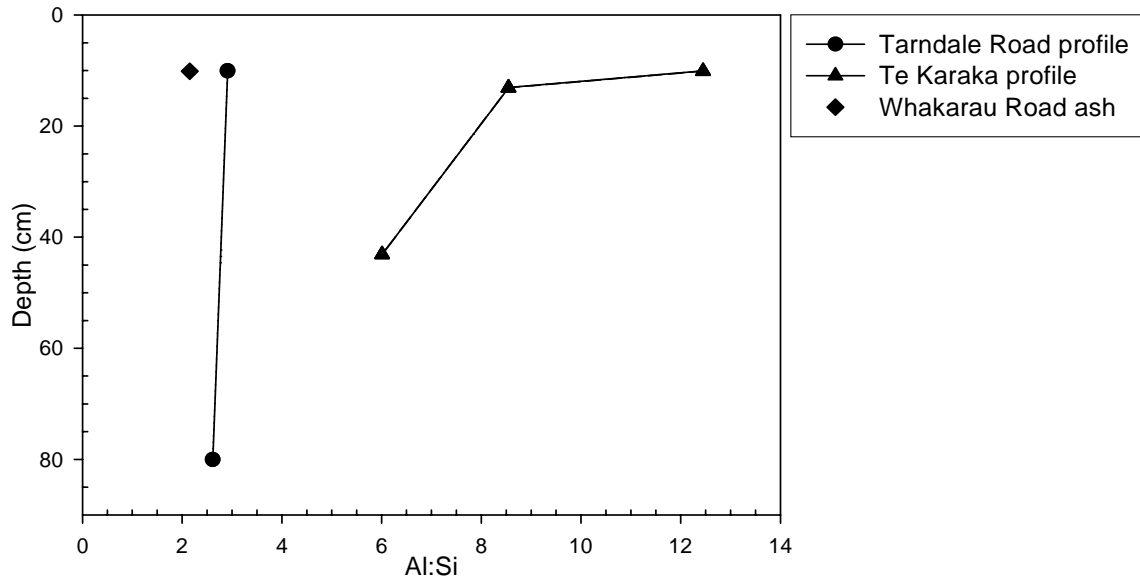


Figure 3.17 Depth and Al:Si relationships from soil and ash profiles from samples collected at the Te Karaka, Tarndale and Whakarau Road localities.

The Al:Si for Tarndale Road profile decreased slightly with increasing depth; however, the Te Karaka profile showed a considerable decrease (~50%) with depth. The Te Karaka topsoil (10 cm) contained the highest concentration of oxalate-extractable Al, perhaps indicating that the extracted Al in this layer was bound to organic complexes. The topsoil was very dark gray in color, in sharp contrast to the white ash layer below that showed the distinct horizonation. The ash (13 cm) had a low %Si<sub>o</sub>, which could be explained by its proximity to the surface or state of development; the Al and Si concentrations may be related to the leaching of these elements, or the Al may be associated in Al-organic complexes. The Te Karaka subsoil (43 cm) maintained dissolved Al and Si concentrations similar to the 13 cm tephra layer.

### **3.4 Particulate Organic Carbon**

In association with the clay mineralogy, the mineral-bound organic carbon (OC) was measured and characterized for this study.  $\delta^{13}\text{C}$  values for the soil and rock samples fall in a fairly wide range, from about -24.2 and -27‰, indicating no clearly distinctive end member values can be assigned (Figure 3.18). The  $\delta^{13}\text{C}$  values of the bulk and <2  $\mu\text{m}$  fractions are relatively well correlated, arguing that the clays reflect the OC composition of the sources as a whole. Another interesting observation is that the bulk OC contents of the rocks are low, and taken at face value, the contents suggest that rocks cannot account for more than about half of the OC in either of the river suspensions. The clay fractions of the rocks, however, have OC values that are very close to those of material suspended in the river. Bulk C/N values of the rivers and shelves fall in the range of soil and rock values. Differences in C/N

are observed in the  $<2\mu\text{m}$  fraction where the rocks and rivers more closely resemble one another. C/N values of the  $<2\mu\text{m}$  fraction of the shelves are similar to the rivers.

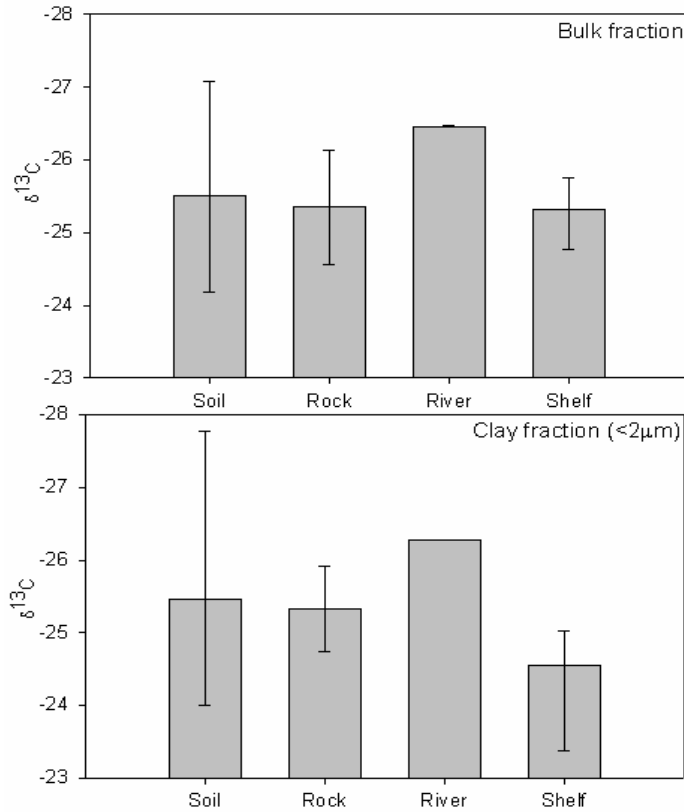


Figure 3.18 Ranges of  $\delta^{13}\text{C}$  values of bulk and  $<2\mu\text{m}$  clay fractions according to sample type.

Organic material peaks were visible in FTIR spectra for the Tarndale Road and Te Karaka soil profiles (Figure 3.19). It was strictly within the topsoils sampled where higher OC concentrations and organic peaks were clearly visible within FTIR; no peaks were clearly distinguishable in the spectra from the river suspensions or shelf sediments. The clay fraction of the Te Karaka topsoil has a %OC of 5.99 as determined by elemental analysis, and in FTIR a signature for organic material (aliphatic C-H) is found in the range of  $3000\text{-}2800\text{ cm}^{-1}$  where N-H and CH stretching occur (Wilson, 1994). The peaks present in this range are  $2924$  and  $2853\text{ cm}^{-1}$ . There was no significant detectable presence of organic matter found in the ash layer (13 cm) or the deep soil layer at 43 cm deep. The Tarndale Road topsoil clay

fraction has a 13.90 %OC identified by C analysis, and a visible area for organics can be seen in FTIR between 3000-2800  $\text{cm}^{-1}$ . Using the Omnic FTIR software, key peaks for C-H and N-H stretching are present at 2924 and 2852  $\text{cm}^{-1}$ . This area is much more prevalent in the topsoil than the ash layer (not shown). The same region in the ash layer has a peak centered at 2928  $\text{cm}^{-1}$ . As expected, %OC in the bulk and clay fractions significantly decreased with depth as microbial activity works to break down the organic matter at depths in the soil. The ash deposits, where the presence of allophane may protect the OC from degradation, still exhibited a %OC of 1.33 or higher.

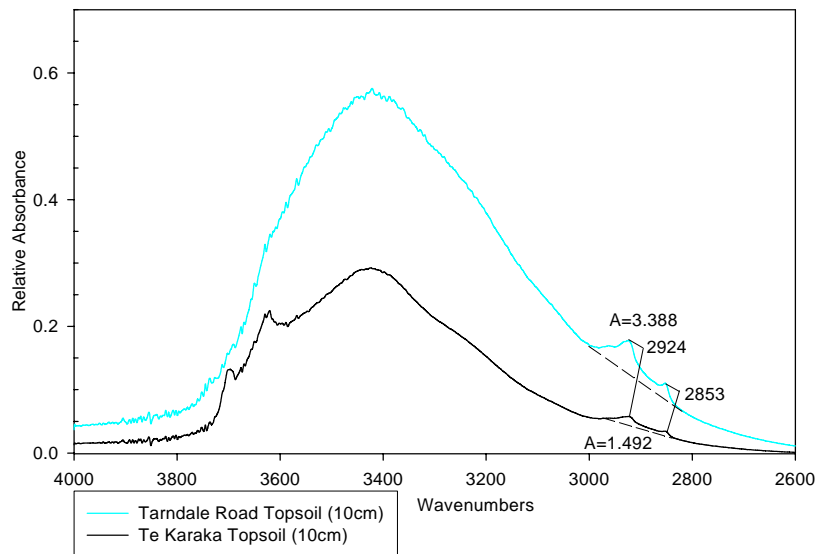


Figure 3.19 OC peaks present in FTIR for the Tarndale Road and Te Karaka topsoils. Associated peaks are 2924 and 2853  $\text{cm}^{-1}$  for aliphatic C-H, with peak area for the Tarndale Road topsoil to be 3.388 and the Te Karaka topsoil to be 1.492.

The young, ashy soils exhibit more positive changes in  $\delta^{13}\text{C}$  values in the clay fraction with depth when compared to the bulk fraction. The finer POC sorbed to the clay particles is better preserved and less accessible to weathering agents than the POC in the bulk fraction. The river suspensions show a mixed OC composition from the rocks and soils. The

OC concentrations of the suspended river solids are comparable to the rocks and the same holds true for the C/N. The data are consistent with the conclusions reached by Leithold et al. (2006) based on  $\delta^{13}\text{C}$  and  $\Delta^{14}\text{C}$ . Further evidence to support this comes from XRD and FTIR analysis where mineralogical signatures denoted the mixing of these different materials. The %OC for the river suspension is fairly low, in the clay fraction range of the two rocks sampled. It is important to note that this shows enrichment in the concentration of finer grain fractions traveling in suspension, which contain more OC, while the coarser material moves as bedload.

The shelf off the Waipaoa provides a record of episodic terrestrial inputs caused by storm events. Gomez et al. (2004) stated that material derived from the gully complexes had more negative  $\delta^{13}\text{C}$  values while landslides were more positive and flood deposits on the margin have a more negative  $\delta^{13}\text{C}$  due to the alternating timing and magnitude relating to the gully and landslide contributions. My study supports research from Gomez et al. (2004) with the Cyclone Bola flood deposit on the shelf off the Waipaoa River to be more negative in  $\delta^{13}\text{C}$ . As expected, both C/N and  $\delta^{13}\text{C}$  support the idea that marine samples are heavily influenced by terrestrial sources. The flood layer (U2303 18-19 cm) shows a somewhat stronger terrestrial influence than the sediments above and below; this holds true for the bulk and  $<2\ \mu\text{m}$  fractions.

Table 3.5 Summarized OC data for bulk and clay (< 2 µm) fractions.

| Sample  | %OC<br>bulk | C/N<br>bulk | δ <sup>13</sup> C<br>Bulk<br>(‰) | %OC<br>< 2 µm | C/N<br>< 2 µm | δ <sup>13</sup> C<br>< 2 µm<br>(‰) |
|---|-------------|-------------|----------------------------------|---------------|---------------|------------------------------------|
| <b>Soils and Ashes</b>                        |             |             |                                  |               |               |                                    |
| Te Karaka topsoil (10 cm)                     | 2.923       | 13.187      | -24.176*                         | 5.991         | 11.023        | -24                                |
| Te Karaka ash (13 cm)                         | 1.466       | 11.935      | -24.273*                         | 1.333         | 8.654         | -25.461*                           |
| Te Karaka subsoil (43 cm)                     | 0.2339      | 5.638       | -27.086*                         | 0.489         | 6.188         | -24.06                             |
| Tarndale Road topsoil (10 cm)                 | 4.724       | 14.928      | -27.038*                         | 13.9          | 13.046        | -26.83                             |
| Tarndale Road ash (80 cm) TD040609-6          | 0.9739      | 19.969      | -24.872*                         | 2.342         | 14.388        | -24.617*                           |
| Whakarau Road ash (near surface)              | 0.3234      | 22.458      | -25.663*                         | 2.979         | 24.719        | -27.772*                           |
| <b>Rocks</b>                                  |             |             |                                  |               |               |                                    |
| Whangai Fm. Mudstone                          | 0.2918      | 9.054       | -25.86                           | 0.8825        | 8.243         | -25.91                             |
| Tikihore Fm. Sandstone                        | 0.3957      | 13.989      | -24.57                           | 0.5069        | 9.084         | -24.74                             |
| <b>Suspended River Solids</b>                 |             |             |                                  |               |               |                                    |
| Waipaoa River suspension (4.83 m)             | 0.7458      | 14.057      | -26.478*                         | 0.705         | 8.649         | -26.27                             |
| Waiapu River suspension (5.40 m)              | 0.6063      | 13.682      | -26.447*                         | 0.6273        | 9.252         | -26.272*                           |
| <b>Shelf Sediments</b>                        |             |             |                                  |               |               |                                    |
| Waiapu shelf sediment, MC3, 43 mwd (1-2 cm)   | 0.4933      | 16.396      | -25.757*                         | 0.7136        | 10.525        | -24.849*                           |
| Waiapu shelf sediment, MC10, 117 mwd (1-2 cm) | 0.6639      | 12.698      | -24.769*                         | 0.894         | 9.149         | -23.382*                           |
| Poverty Bay Core U2303 (4-6 cm)               | 0.1494      | 8.032       | -25.14                           | 0.6139        | 7.879         | -24.62                             |
| Poverty Bay Core U2303 (18-19 cm)             | 0.8962      | 11.316      | -25.58                           | 0.6927        | 8.401         | -25.03                             |
| Poverty Bay Core U2303 (31-33 cm)             | 0.1684      | 8.085       | -25.31                           | 0.5419        | 7.834         | -24.9                              |

C/N refers to atomic C/N, δ<sup>13</sup>C is corrected values; \* refers to samples collected by dual inlet method.

#### **4. DISCUSSION**

Research conducted on the Waipaoa and Waiapu Rivers on the North Island of New Zealand has recognized and characterized geomorphologic and geochemical processes responsible for the control and delivery of sediment and associated OC to the adjacent margin. Rocks, soils and widespread tephra deposits contribute large volumes of sediment to the rivers from deeply incised gullies, sheetwash, earthflows and landslides within the catchments (Mazengarb and Speden, 2000; Glade, 2003; Gomez et al., 2003 a, b, 2004; Orpin, 2004; Leithold et al., 2006). Gully erosion accounts for 50% of the sediment generated in the Waipaoa and 70% in the Waiapu, and provides a fairly continuous source of sediment to the river (Blair et al., 2004; Leithold et al., 2006). The relationship between sedimentary formations and clay mineral compositions shows that the compositions are characteristic of the depositional environments. The bedrock is suspected to have originated in a shallow marine environment where burial led to low grade metamorphism (Weaver, 1989; Churchman et al., 1991; Mazengarb and Speden, 2000; Laird et al., 2003). This low temperature and pressure regime led to the formation of index minerals such as chlorite. Uplift and weathering of the bedrock release chlorite and other clays. The high erosion rates, short residence times in the river, and rapid burial in the marine environment contribute to the preservation of chlorite, making it a characteristic bedrock-derived mineral. Soils in the Waipaoa provide a significant input of clay minerals to the river and continental shelf.

XRD and FTIR of the rocks revealed well structured clay minerals that showed little absorbed water on the mineral structure. The sharp peaks in both XRD and FTIR are indicative of this. Results from the volcanic soils, however, produced spectra that showed more hydration and absorbed water possibly due to weathering processes and the breakdown

of crystalline minerals. More interstratified minerals were found in the soils. The ash samples exhibited the most variability in XRD with no distinct mineral compositions being noted. This could be attributed to compositional differences with poorly ordered minerals (i.e. allophane) and volcanic glass. Allophane was identified in the ash samples by FTIR based on the diagnostic peaks and also by the amount of hydration of the samples throughout the entire scan range. XRD revealed 50% or more of the clay composition of the sampled bedrock consisted of illite but was also detected in the soil in lesser quantities. Chlorite was established as a diagnostic mineral derived from the weathering of the bedrock while smectite characterized the volcanic soils (Figure 3.1, Table 3.3). River suspension compositions were consisted primarily of illite and chlorite suggesting that the rocks contribute a significant quantity (up to half) of the material being transported by the river. However, the volcanic soils contribute a large quantity of material to the Waipaoa River (Table 3.3). The presence of interstratified clay minerals in the river suspensions could be attributed to the addition of soils from erosion processes within the watersheds.

In addition to clay minerals forming from the weathering of bedrock, tephra deposits from episodic volcanic eruptions contribute its own unique assemblage of clay minerals. Volcanic soils, or Andisols, possess a unique set of chemical and physical properties that include low bulk density, volcanic glass, high phosphorous retention, high organic matter content, and the presence of poorly crystalline minerals such as allophane, imogolite, and ferrihydrite formed by *in situ* transformations (Haantgens and Bleeker, 1970; Lowe, 1986; Chamley, 1989; Parfitt, 1990; Buol et al., 2003; Rasmussen et al., 2007). Allophane and imogolite have been described as meta-stable, short-range ordered to poorly crystalline hydrous aluminosilicate clay minerals ( $\text{Al}_2\text{SiO}_4 \cdot n\text{H}_2\text{O}$ ) having Al:Si ratios ranging from 1.0-

2.0, controlled by environmental factors (Wada, 1977; Stevens and Vucetich, 1985; Lowe, 1986; Parfitt, 1990, Ohashi et al., 2005). Allophane exists as hollow spherules or fibrous and tubular structures as revealed by SEM. The hollow spherule structure of allophane has a diameter of 3-5 nm with the predominant bonding of Si-O-Al (Lowe, 1986; Parfitt, 1990; Martínez et al., 2001). Al-rich allophane can have a fibrous structure related to imogolite (Al:Si = 2:1) and has been termed proto-imogolite allophane (Parfitt, 1990).

The incorporation of a synthetic allophane standard, created according to the methods of Ohashi et al. (2002), provided assistance in the recognition of allophane in the Waipaoa catchment through FTIR. Studies of allophane in FTIR reveal broad, unresolved OH stretching bands and the associated absorbed water and hydration of the mineral structure help to identify allophane. Although the soil and ash samples contained a mixed mineral assemblage, characteristic allophane peaks were found within these samples based on broad diagnostic peaks within the OH stretching regions.

A number of factors including precipitation, age, burial depth and thickness of the ash layers could explain the differences between Te Karaka, Tarndale Road and Whakarau Road results. Any of these factors or combination thereof may regulate the breakdown of the volcanic ash and the transformations of allophane to more stable minerals. The Tarndale ash is suspected to be from a Waimihia eruption ( $3280 \pm 20$  ybp) based on its depth and reports of widespread distribution (Eden et al., 2001) and shows the most mineralogic development noted by the more refined peaks in FTIR (Figure 3.8). The pumiceous, near surface Te Karaka and Whakarau Road ashes likely originated from a Taupo eruption ( $1850 \pm 10$  ybp). The Whakarau Road ash layer, sampled near the upper surface of the deposit, presents one of the thicker depositional units (being over a meter thick). The Whakarau Road ash layer was

the only deposit that contained a recognizable signature for allophane, while the Te Karaka ash more closely resembled the soil horizons above and below it. The presence of kaolinite in the Te Karaka and Tarndale ashes could obscure a positive identification of allophane. Typically seen in soil profiles is clay mineral maturity decreasing with depth (Martini and Chesworth, 1992), but the opposite is seen in the Te Karaka profile. In this profile, we see increasing mineral development with depth. This could be explained by the addition of tephra deposits which cover the land and thus bury the soil below. These events interrupt the weathering process to the soil below and, in a sense, reset the record for soil and mineral development.

Some volcanic soils are noted for their high OC content due to the function of allophane in sorbing OM and declines with the accumulation of more crystalline minerals during pedogenesis (Percival et al., 2000; Kleber et al., 2005; Mikutta et al., 2005). In volcanic soils, biochemical and enzyme activities between organic matter and allophane are low, but once complexes are formed, they account for slower rates of mineralization of C and N in the soils (Parfitt, 1990). It has also been suggested that allophane rich soils are associated with having high free-Al content, and this subsequent Al-toxicity may protect the OC from being degraded (Martínez et al., 2001; Kahle et al., 2004; Rasmussen et al., 2006). The burial depth and thickness of the tephra deposit are other contributing factors controlling the mineralogy, formation of allophane and the organic matter content (OM, humus complexes) (Lowe, 1986). The depth of burial in soils controls the organic matter content because burial limits the amount of organic matter inputs and, over time, the humus complexes break down.

Geochemical signatures and stable organic carbon isotopic compositions ( $\delta^{13}\text{C}$ ) help characterize the sources actively contributing POC back into the C cycle during weathering, fluvial mixing, transportation, and deposition on the continental margins (Leithold and Hope, 1999; Gomez et al., 2004a; Leithold et al., 2006).  $\delta^{13}\text{C}$  compositions in the Te Karaka profile yielded interesting results, showing heavy (positive) values in the two uppermost samples and more negative values at depth. This suggests the possibility of vegetation changes (C3 to C4 plants) as a result of the landscape alterations. Further research would be required to make better interpretations to the relationship effects of C3 and C4 plants and the soils. Leithold et al. (2006) noted that times of low yields carry the signatures of modern plant derived OC which can be attributed to sheet wash and shallow landsliding while high yield events with material generated from gullies show older OC coming from the rocks. Data from these high yield events indicate  $\delta^{13}\text{C}$  values that are more positive and have values that approach the rocks within the watershed (Gomez et al., 2004a; Leithold et al., 2006).

Episodic, intense storm events produce landslides which generate large amounts of sediment being delivered to the rivers and shelf. While no detectable signatures for allophane could be clearly identified in the river suspensions, the techniques used in this research helped identify allophane in the flood layer (Core U2303, 18-19 cm, Figure 3.14) as well. This discovery provides documented evidence of terrigenous material (soils, and more importantly, volcanic deposits) being preserved on the shelf. The discovery of allophane in the flood layer indicates that allophane can persist when it is accompanied by the deposition of large volumes of sediment in a shelf environment.

The geomorphologic processes responsible for generating the sediment being transported by the river to the continental shelf include gully erosion and landsliding. The

gully erosion supplying the majority of sediment is a more chronic problem whereas landslides are often triggered by high intensity storms and periods of prolonged rainfall. The shelf off the Waipaoa provides a record of episodic terrestrial inputs caused by storm events. Gomez et al. (2004) stated that material derived from the gully complexes into bedrock had more negative  $\delta^{13}\text{C}$  values than the soils eroding during shallow landsliding. Gomez et al. (2004) also found a negative  $\delta^{13}\text{C}$  value for Cyclone Bola sediments deposited on the floodplain early in the event and interpreted those sediments to have been derived primarily from gullies. They speculated, however, that later in the storm, more of the sediment would have been derived from landsliding and would be expected to have a more positive  $\delta^{13}\text{C}$  value associated with soil-derived material. The  $\delta^{13}\text{C}$  values measured in the shelf sediments could record different contributions from rocks and soils. Another alternative interpretation is that the flood layer is more negative because it was deposited rapidly and less marine carbon ( $\delta^{13}\text{C}$  about -21‰) has been incorporated into it than into the sediments above and below. However, with the limited data of this research, more samples and analyses are required to provide further insight to these processes.

## **5. CONCLUSIONS**

a. Two rocks that represent the predominant lithologies in the watershed were examined—a mudstone and a sandstone. The rocks both contain illite, chlorite, smectite, and kaolinite. The mudstone is composed mostly of illite with equal amounts of kaolinite and chlorite and lesser amounts of smectite. The sandstone contains more chlorite and kaolinite than the mudstone but significantly less smectite. Interstratified illite and smectite is revealed by FTIR.

b. Soils from two localities contain fewer crystalline clay minerals than the rocks, and those clay minerals present are more hydrated, indicating volcanic sources.

c. The Tarndale topsoil and a buried ash layer in the profile contain weakly crystalline to disordered kaolinite, and smectite. Illite and mixed-layer chlorite-smectite is also present.

d. The Te Karaka soil samples contain kaolinite, illite, smectite, and interstratified illite-smectite. The kaolinite is disordered. Allophane is present in all three samples from this site (topsoil, ash layer, subsoil).

e. Ash layers from three localities in the Waipaoa watershed all show low crystallinity, with allophane dominant in the Tarndale and Whakarau Road ashes.

f. Samples of suspended solids from the Waipaoa and Waiapu Rivers contain chlorite, kaolin, illite, smectite, and interstratified illite-smectite. Smectite is the dominant mineral in suspension in the Waipaoa while illite is principal mineral in the Waiapu. The Waipaoa contains more kaolinite than the Waipaoa.

g. Evidence that the river suspension contains material from both bedrock and soils includes sharper peaks in the FTIR spectra between  $1100\text{-}400\text{ cm}^{-1}$  indicating the contributions of well ordered clays from bedrock, and more absorbed water and Si-OH and H<sub>2</sub>O stretching between  $4000\text{-}2800\text{ cm}^{-1}$ , resembling patterns observed in soil samples.

h. The sediment being deposited on the continental margins adjacent to the Waipaoa and Waiapu Rivers is composed of illite, smectite, chlorite, and kaolinite. These samples bear signatures resembling material from the river suspensions. FTIR reveals the clays in the shelf sediments have more absorbed water, similar to what is seen in the soil samples. However, the absorbed water may be explained by the clay mineral residence in the seabed.

i. Flood layers in continental shelf environments are a result of storm events that drive the geomorphologic processes within the watersheds. Poverty Bay Core U2303 has a 10 cm thick flood layer from Cyclone Bola that provides documented evidence of volcanic soils being deposited. Allophane was identified in this flood layer and its presence suggests that the deposition of large volumes of sediment can preserve this meta-stable mineral.

j. Sediment taken from two cores across the Waiapu shelf show small changes in mineralogy. Chlorite content increased and illite content decreased with progression across the shelf. Kaolinite and smectite were also identified.

k. The Tarndale and Whakarau Road ash layers contained the highest percentage of dissolvable Al and Si; this can be attributed to the presence of allophane (which was identified in FTIR). The Te Karaka soil expressed changes down the profile. The weathering of the volcanic glass and the thickness of the tephra bed would yield the higher concentrations of dissolvable Al and Si as seen in these profiles. Al:Si values for the ash layers fall in the ranges discussed in the literature indicating allophane is in these layers.

l. Rock and soil  $\delta^{13}\text{C}$  values fall in a fairly wide range, from about -24.2 and -27‰, which do not allow for the assignment of clearly distinctive end member values. However, the relatively well correlated  $\delta^{13}\text{C}$  values of the bulk and  $<2\ \mu\text{m}$  fractions indicate that the clays reflect the OC composition of the sources as a whole. It is also important to note that even though the bulk OC contents of the rocks are low, the contents suggest that rocks cannot account for more than about half of the OC in either of the river suspensions.

m. Organic matter peaks were visible in FTIR spectra for the Tarndale Road and Te Karaka topsoil samples. In FTIR a signature for organic material (aliphatic C-H) is found in the range of  $3000\text{-}2800\ \text{cm}^{-1}$  where N-H and CH stretching occur. There was no significant detectable presence of organic matter found in the ash layers, river suspensions, and shelf sediment.

n. A significant quantity of the fine fraction traveling in Waipaoa and Waiapu suspensions is clays. The %OC and C/N of the river suspension is comparable to the rocks, but evidence to support a mixed input from the rocks and soil comes from mineralogical signatures.

o. Flood deposit  $\delta^{13}\text{C}$  and C/N support the idea that marine samples are heavily influenced by terrestrial sources. The flood layer (U2303 18-19 cm) bulk and clay fractions show a somewhat stronger terrestrial influence than the sediments above and below.

In the Waipaoa and Waiapu catchments, erosion occurs primarily through gullies deeply incised in the bedrock and by shallow landslides. The large amounts of material derived from the gullies and landslides, transported and eventually deposited onto the continental margin include fresh and weathered bedrock, soils, and tephra deposits. By first identifying clay minerals that are distinctive of these sources, interpretations of the influence of these sources and the geomorphologic processes controlling sedimentary behavior can be better understood.

This research utilized XRD to determine initial clay mineral compositions, then complimented and confirmed the clay mineralogy with FTIR. XRD is an invaluable tool for clay mineral identification due to its consistency and the reproducibility of the results. One disadvantage to using this method involved the time in preparing and processing the samples for analysis. XRD works very well for the identification of clays with a regular, repeating structure, but poorly crystalline clays have less recognizable signatures. FTIR is beneficial because it's ability in determining clay minerals with varying degrees of structure because the amount of sample required is very small, the time required for data collection, and the reproducibility of the results.

Since identifying chlorite as a primarily rock-derived mineral and smectite being the dominant soil-derived mineral in the catchments, the geomorphologic processes responsible for contributing sediment can be more readily recognized. Sampling the rivers during varying flow conditions can aid in a more accurate quantification of particulates from the sources. This research also examined surface layers for spatial variability and one core to examine temporal variability in clay mineralogy. Long-term sediment preservation would require more downcore studies over a wider area to investigate temporal and spatial trends in sediment deposition across the shelf.

## **REFERENCES**

Basile-Doelsch, I., R. Amundson, W.E.E. Stone, C.A. Masiello, J.Y. Bottero, F. Colin, F.

Masin, D. Borschneck and J.D. Meunier, 2005. Mineralogical control of organic carbon dynamics in a volcanic ash soil on La Réunion. *European Journal of Soil Science* 56, p. 689-703.

Bertaux, J., F. Fröhlich, and P. Ildefonse, 1998. Multicomponent analysis of FTIR spectra: quantification of amorphous and crystallized mineral phases in synthetic and natural sediments. *Journal of Sedimentary Research* 68, p. 440–447.

Biscaye, P.E., 1965. Mineralogy and sedimentation of recent deep-sea clays in the Atlantic Ocean and adjacent seas and oceans. *Geological Society of America Bulletin* 76, p. 803–831.

Blair, N.E., and W.D. Carter, 1992. The carbon isotope geochemistry of acetate from methanogenic marine sediment. *Geochimica et Cosmochimica Acta* 56, p. 1247-1258.

Blair, N.E., E.L. Leithold, S.T. Ford, K.A. Peeler, J.C. Holmes, and D.W. Perkey, 2003. The persistence of memory: The fate of ancient sedimentary organic carbon in a modern sedimentary system. *Geochimica et Cosmochimica Acta* 67, 63-73.

Blair, N.E., E.L. Leithold, R.C. Aller, 2004. From bedrock to burial: the evolution of particulate organic carbon across coupled watershed-continental margin systems. *Marine Chemistry* 92, p. 141-156.

Brackely, H.L., 2006, Land to ocean transfer of erosion-related organic carbon, Waipaoa sedimentary system, East Coast New Zealand, Ph.D. thesis, Victoria University, Wellington, 129 pp.

- Brady, N.C. and R.R. Weil, 2000. Elements of the Nature and Properties of Soils. Prentice Hall Inc., New Jersey.
- Broquen, P., J.C. Lobartini, F. Candan, and G. Falbo, 2005. Allophane, aluminum, and organic matter accumulation across a bioclimatic sequence of volcanic ash soils of Argentina. *Geoderma* 129, 167-177.
- Buol, S.W., R.J. Southard, R.C. Graham, and P.A. McDaniel, 2003. *Soil Genesis and Classification*. 5 ed., Iowa State Press: Iowa.
- Carter, M.R., ed. 1993. *Soil Sampling and Methods of Analysis*. Lewis Publishers, Boca Raton.
- Certini, G., M.J. Wilson, S.J. Hillier, A.R. Fraser, E. Delbos, 2006. Mineral weathering in trachydacitic-derived soils and saprolites involving formation of embryonic halloysite and gibbsite at Mt. Amiata, Central Italy. *Geoderma* 133, p. 173–190.
- Chamley, H., 1989. *Clay Sedimentology*. Springer-Verlag, Berlin.
- Churchman, G.J., P.D. McIntosh, C.M. Burke, J.S. Whitton, 1991. Clay mineralogy of soils formed in tuffaceous greywacke, Southland, New Zealand, in relation to genesis, soil properties and classification. *Australian Journal of Soil Research* 29, 493-513.
- Dixon, J.B. and G.N. White, 1997. *Soil Mineralogy Laboratory Manual—Agronomy 626*. (Published by the authors).
- DeRose, R.C., B. Gomez, M. Marden, and N.A. Trustrum, 1998. Gully erosion in Mangatu Forest, New Zealand, estimated from digital elevation models. *Earth Surface Processes and Landforms* 23, 1045-1053.

- Eden, D.N., A.S. Palmer, S.J. Chronin, M. Marden, K.R. Berryman, 2001. Dating the culmination of river aggradation at the end of the last glaciation using distal tephra compositions, eastern North Island, New Zealand. *Geomorphology* 38, 133-151.
- Essington, M.E., 2004. *Soil and Water Chemistry: an integrative approach*. CRC Press, Boca Raton.
- Farmer, V.C. and J.D. Russell, 1966. Infrared absorption spectrometry in clay studies. Fifteenth National Conference on Clays and Clay Minerals. *Clays and Clay Minerals*.
- Farmer, V.C, A.R. Fraser, J.D. Russell, and N. Yoshinaga, 1977. Recognition of imogolite structures in allophanic clays by infrared spectroscopy. *Clay Minerals* 12, 55-57.
- García-Rodeja, E., J.C. Nóvoa, X. Pontevedra, A. Martínez-Cortizasa, and P. Buurman, 2004. Aluminum fractionation of European volcanic soils by selective dissolution techniques. *Catena* 56, 155-183.
- Glade, T., 2003. Landslide occurrence as a response to land use change: a review from New Zealand. *Catena* 51, 297-314.
- Gomez, B., K. Banbury, M. Marden, N.A. Trustrum, D.H. Peacock, and P.J. Hoskin, 2003a. Gully erosion and sediment production: Te Weraroa Stream, New Zealand. *Water Resources Research* 39, 1187-1193.
- Gomez, B., N.A. Trustrum, D.M. Hicks, K.M. Rogers, M.J. Page, and K.R. Tate, 2003b. Production, storage, and output of particulate organic carbon: Waipaoa River Basin, New Zealand. *Water Resources Research* 39, 1161-1168.
- Gomez, B., H.L. Brackley, D.M. Hicks, H. Neff, and K.M. Rogers, 2004a. Organic carbon in floodplain alluvium: Signature of historic variations in erosion processes associated

- with deforestation, Waipaoa River Basin, New Zealand. *Journal of Geophysical Research* 109, F04011.
- Gomez, B., L. Carter, N.A. Trustrum, A.S. Palmer, A. P. Roberts, 2004b. El Nino-Southern Oscillation signal associated with middle Holocene climate change in intracorrelated terrestrial and marine sediment cores, North Island, New Zealand. *Geology* 32, 653-656.
- Haantgens, H.A. and P. Bleeker, 1970. Tropical weathering in the territory of Papua and New Guinea. *Australian Journal of Soil Research* 8, 157-77.
- Hedges, J.I. and J.M. Oades, 1997. Comparative organic geochemistries of soils and marine sediments. *Organic Geochemistry* 27, 319-361.
- Hicks, D.M., B. Gomez, and N.A. Trustrum, 2000. Erosion thresholds and suspended sediment yields, Waipaoa River Basin, New Zealand. *Water Resources Research* 36, 1129-1142.
- Hicks, D.M., B. Gomez, and N.A. Trustrum, 2004. Event suspended sediment characteristics and the generation of hyperpycnal plumes at river mouths: East Coast Continental Margin, North Island, New Zealand. *Journal of Geology* 112, 471-485.
- Kahle, M., M. Kleber, and R. Jahn, 2003. Retention of dissolved organic matter by phyllosilicate and soil clay fractions in relation to mineral properties. *Organic Geochemistry* 35, 269-276.
- Kao, S.J., and K.K. Liu, 1996. Particulate organic carbon export from a subtropical mountainous river (Lanyang Hsi) in Taiwan. *Limnology and Oceanography* 41, 1749-1757.

- Kasai, M., G.J. Brierley, M.J. Page, T. Marutani, N.A. Trustrum, 2005. Impacts of land use change on patterns of sediment flux in Weraamaia catchment, New Zealand. *Catena* 64, 27-60.
- Kennedy, M.J., D.R. Pevear, and R.J. Hill, 2002. Mineral surface control of organic carbon in black shale. *Science* 295, 657-660.
- Keil, R.G., E. Tsamakis, C. Bor Fuh, J.C. Giddings, and J.I. Hedges, 1994, Mineralogical and textural controls on the organic composition of coastal marine sediments: hydrodynamic separation using SPLITT fractionation: *Geochimica et Cosmochimica Acta* 58, 879-893.
- Keil, R.G. and J.I. Hedges, 1993. Sorption of organic matter to mineral surfaces and the preservation of organic matter in coastal marine sediments. *Chemical Geology* 107, p. 385-388.
- Kleber, M., R. Mikutta, M.S. Torn, and R. Jahn, 2005. Poorly crystalline mineral phases protect organic matter in acid subsoil horizons. *European Journal of Soil Science* 56, 717-725.
- Komada T., E.R.M. Druffel, and S.E. Trumbore, 2004. Oceanic export of relict carbon by small mountainous rivers. *Geophysical Research Letters* 31, L07504.
- Laird, M.G., K.N. Bassett, P. Schioler, H.E.G. Morgans, J.D. Bradshaw, and S.D. Weaver, 2003. Paleoenvironmental and tectonic changes across the Cretaceous/Tertiary boundary at Tora, southeast Wairarapa, New Zealand: a link between Marlborough and Hawke's Bay. *New Zealand Journal of Geology & Geophysics* 46, 275-293.
- Leithold, E.L., and N.E. Blair, 2001. Watershed control on the carbon loading of marine sedimentary particles. *Geochimica et Cosmochimica Acta* 65, 2231-2240.

Leithold, E.L., N.E. Blair, and D.W. Perkey, 2006. Geomorphologic Controls on the Age of Particulate Organic Carbon from Small Mountainous and Upland Rivers. *Global Biogeochemical Cycles* 20, GB3022.

Leithold, E.L., and R.S. Hope, 1999. Deposition and modification of a flood layer on the northern California shelf: lessons from and about the fate of terrestrial particulate organic carbon. *Marine Geology* 154, 183-195.

Lowe, D.L., 1986. Controls on the rates of weathering and clay mineral genesis in airfall tephra: a review and New Zealand case study. In "Rates of chemical weathering of rocks and minerals." Eds. S.M. Coleman and D.P. Dethier. Academic Press: New York.

Madejová, J. and P. Komadel, 2001. Baseline Studies of the Clay Minerals Society Source Clays: Infrared Methods. *Clays and Clay Minerals* 49, 410-432.

Martínez, C.E., A. Jacobson, and M.B. McBride, 2001. Thermally induced changes in metal solubility of contaminated soils is linked to mineral recrystallization and organic matter transformations. *Environmental Science and Technology* 35, 908-916.

Martini, I.P. and W. Chesworth, 1992. *Weathering, Soils, and Paleosols*. Elsevier Science Publishers, New York.

Mazengarb, C. and I.G. Speden, 2000. Geology of the Raukumara Area. Institute of Geological and Nuclear Sciences 1:250,000 geological map 6. 1 sheet and 60 pp. Lower Hutt, New Zealand. Institute of Geological and Nuclear Sciences.

Mikutta, R., M. Kleber, and R. Jahn, 2005. Poorly crystalline minerals protect organic carbon in clay subfractions from acid subsoil horizons. *Geoderma* 128, 106-115.

- Milliman, D.J., and J.P.M. Syvitski, 1992. Geomorphic/tectonic control of sediment discharge to the ocean: The importance of small mountainous rivers. *Journal of Geology* 100, 525-544.
- Moore D.M., and R.C. Reynolds, ed. 1997. X-ray diffraction and the identification and analysis of clay minerals. Oxford; New York. Oxford University Press, 2nd ed.
- Mosser-Ruck, R., K. Devineau, D. Charpentier, and Cathelineau, M., 2005. Effects of ethylene glycol saturation protocols on XRD patterns: A critical review and discussion. *Clays and Clay Minerals* 53, p. 631-638.
- Ohashi, F., S.I. Wada, M. Suzuki, M. Maeda, and S. Tomura, 2002. Synthetic allophane from high concentration solutions: nanoengineering of the porous solid. *Clay Minerals* 37, 451-456.
- Orpin, A.R., 2004. Holocene sediment deposition on the Poverty-slope margin by the muddy Waipaoa River, East Coast New Zealand. *Marine Geology* 209, 69-90.
- Owens, P.N., R.J. Batalla, A.J. Collins, B. Gomez, D.M. Hicks, A.J. Horowitz, G.M. Kondolf, M. Marden, M.J. Page, D.H. Peacock, E.L. Petticrew, W. Salomons, and N.A. Trustrum, 2005. Fine-grained sediment in river systems: environmental significance and management issues. *River Research and Applications* 21, 693-717.
- Page, M.J., L.M. Reid, and I.H. Lynn, 1999; sediment production from Cyclone Bola landslides; Waipaoa catchment. *Journal of Hydrology. New Zealand* 38, 289-308.
- Parfitt, R.L., 1990. Allophane in New Zealand-A Review. *Australian Journal of Soil Research* 29, 343-360.
- Parfitt, R.L., B.K.G. Theng, J.S. Whitton, and T.G. Shepard, 1997. Effects of clay minerals and land use on organic matter pools. *Geoderma* 75, 1-12.

- Parfitt, R.L., M. Russell, and G.E. Orbell, 1983. Weathering sequence of soils from volcanic ash involving allophane and halloysite, New Zealand. *Geoderma* 29, 41-57.
- Parfitt, R.L. and T. Henmi, 1982. Methods for estimating the amount of allophane in soil clays formed from basalt and volcanic ash and in podzolised soils. *Soil Science and Plant Nutrition* 28, 183-190.
- Percival, H.J., R.L. Parfitt, and N.A. Scott, 2000. Factors controlling soil carbon levels in New Zealand Grasslands: Is clay content important? *Soil Science Society of America Journal* 64, 1623-1630.
- Pironon, J., M. Pelletier, P. De Donato and R. Mosser-Ruck, 2003. Characterization of smectite and illite by FTIR spectroscopy of interlayer NH<sub>4</sub><sup>+</sup> cations. *Clay Minerals* 38, p. 201–211.
- Poppe, L.J., V.F. Paskevich, J.C. Hathaway, and D.S. Blackwood, 2001. A Laboratory Manual for X-Ray Powder Diffraction. U.S. Geological Survey Open-File Report 01-041. <http://pubs.usgs.gov/of/2001/of01-041/htmldocs/methods/squant.htm>
- Post, J.L. and L. Borer, 2002. Physical properties of selected illites, beidellites and mixed-layer illite–beidellites from southwestern Idaho, and their infrared spectra. *Applied Clay Science* 22, p. 77– 91.
- Ransom, B., K. Dongseom, M. Kastner, and S. Wainwright, 1998. Organic matter preservation on continental slopes: importance of mineralogy and surface area. *Geochimica et Cosmochimica Acta* 62, 1329-1345.
- Rasmussen, C., R.J. Southard, and W.R. Horwath, 2006. Mineral control of organic carbon mineralization in a range of temperate conifer forest soils. *Global Change Biology* 12, 834-847.

- Raymond, P.A., and J.E. Bauer, 2001. Use of  $^{14}\text{C}$  and  $^{13}\text{C}$  natural abundances for evaluating riverine, estuarine, and coastal DOC and POC sources and cycling: a review and synthesis. *Organic Geochemistry* 32, 469-485.
- Reid, L.M., and M.J. Page, 2002. Magnitude and frequency of landsliding in a large New Zealand catchment. *Geomorphology* 49, 71-88.
- Russell, M., R.L. Parfitt, and G.G.C. Calridge, 1981. Estimation of the amounts of allophane and other materials in the clay fraction of an Egmont loam profile and other volcanic ash soils, New Zealand. *Australian Journal of Soil Research* 19, 185-195.
- Soil Survey Staff, 1999. *Soil Taxonomy—A Basic System of Soil Classification for Making and Interpreting Soil Surveys*. 2nd ed. Agriculture Handbook No. 436. USDA-NRCS, 869.
- Su, Chunming and D. L. Suarez, 1997. Boron Sorption and Release by Allophane. *Soil Science Society of America Journal* 6, 69-77.
- Syvitski, J.P.M., C.J. Vörösmarty, A.J. Kettner, and P. Green, 2005. Impact of Humans on the Flux of Terrestrial Sediment to the Global Coastal Ocean. *Science* 308, 376-380.
- Tate, K.R., N.A. Scott, A. Parshotam, L. Brown, R.H. Wilde, D.J. Giltrap, N.A. Trustrum, B. Gomez, and D.J. Ross, 2000. A multi-scale analysis of a terrestrial carbon budget: Is New Zealand a source or sink of carbon? *Agriculture, Ecosystems and Environment* 82, 229-246.
- Torn, M.S., S.E. Trumbore, O.A. Chadwick, P.M. Vitousek, and D.M. Hendricks, 1997. Mineral control of soil organic carbon storage and turnover. *Nature* 389, 170-173.
- Ugolini, F.C., and R.A. Dahlgren, 2002. Soil development in volcanic ash. *Global Environmental Research* 6, 69-81.

Wada, K., 1977. Allophane and Imogolite. In "Minerals in soil environments." J.B. Dixon and S.B. Weed (Eds.). American Society of Agronomy, Madison, Wisconsin. pp. 603-638.

Weaver, C.E., 1989. Clays, Muds, and Shales. Elsevier Science Publishers, New York.

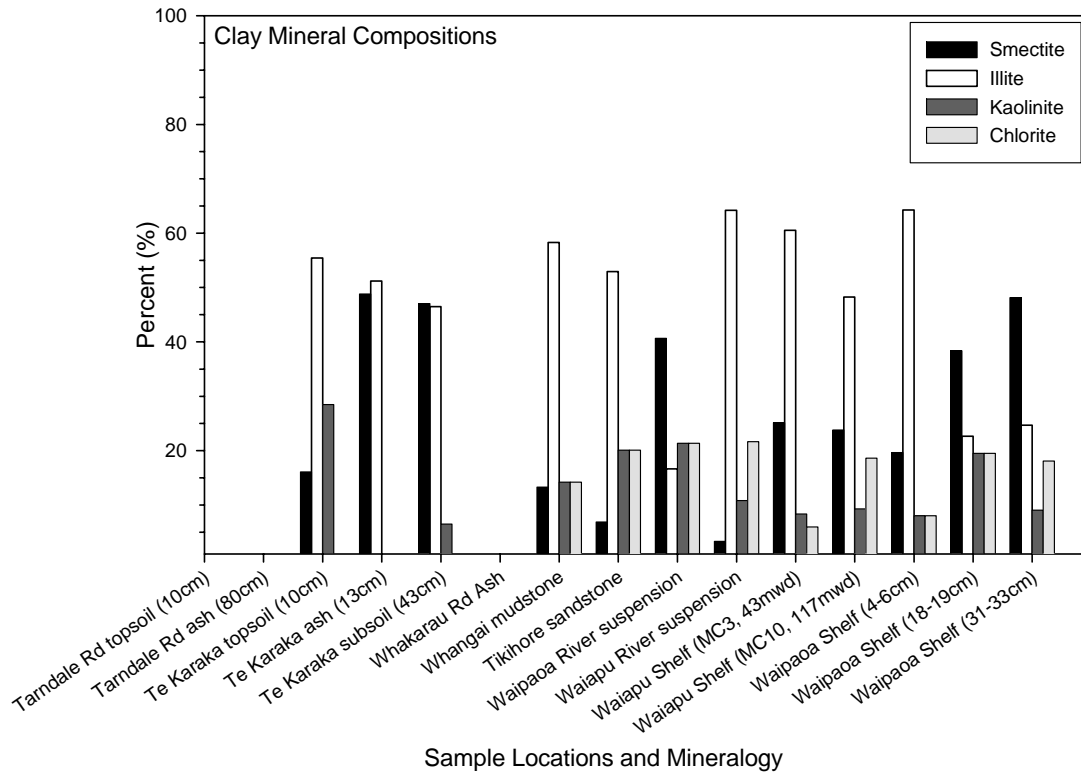
Wilson, M.J., ed. 1994. Clay Mineralogy: Spectroscopic and Chemical Determinative Methods. Chapman and Hall, London.

## **Appendix**

## 7.1 Grain Size Analysis

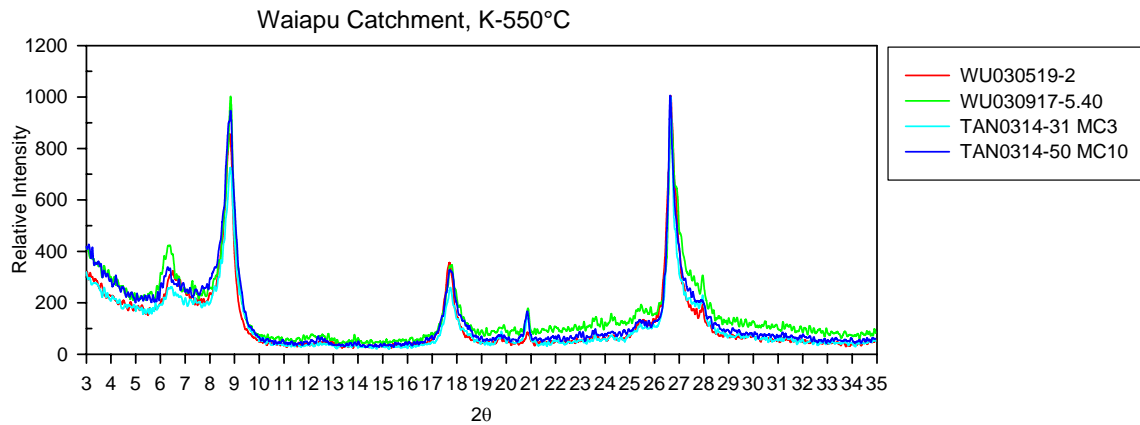
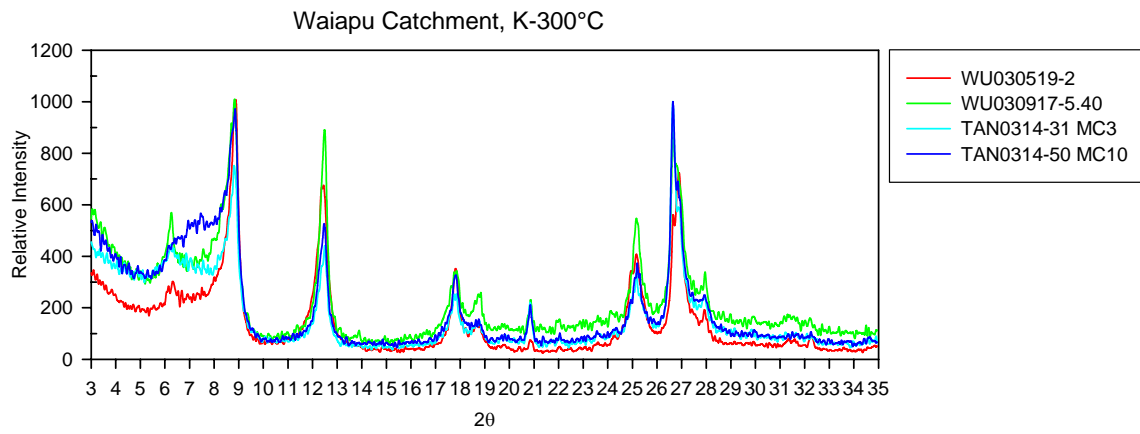
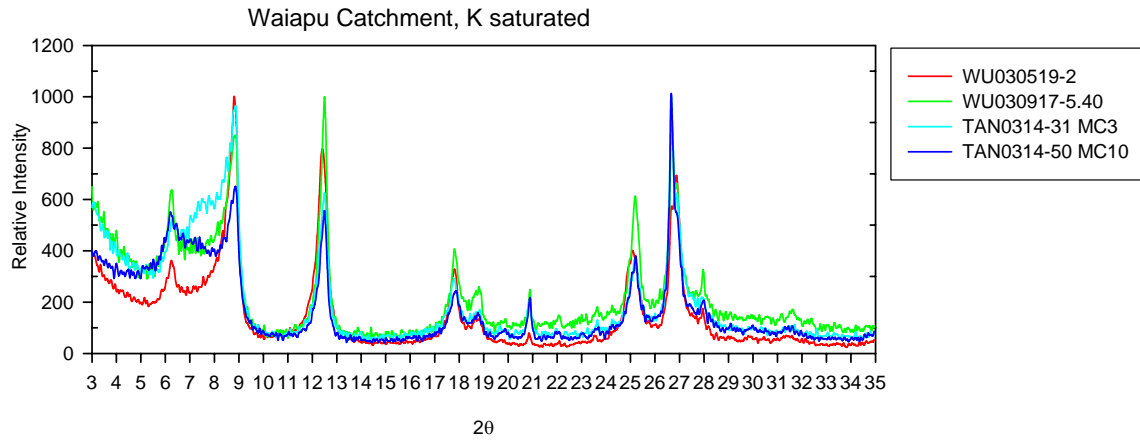
|                          | Depth    | Sample Type    | Total weight of sample | % >25 | % <2    | %>2, <25 |               |
|--------------------------|----------|----------------|------------------------|-------|---------|----------|---------------|
| <b>Waipaoa Catchment</b> |          |                |                        |       |         |          |               |
| TD040609-2               | 10 cm    | Soil           | 14.23                  | 83.99 | 0.26    | 15.75    |               |
|                          |          | Soil           | 11.64                  | 75.90 | 0.74    | 23.36    |               |
| TD040609-6               | 80 cm    | Ash layer      | 13.35                  | 62.14 | No data | No data  | no salt added |
|                          |          | Ash layer      | 18.35                  | 72.04 | 1.71    | 26.25    |               |
| WK030513-7               | 100cm    | Ash layer      | 16.13                  | 85.32 | No data | No data  | no salt added |
|                          |          | Ash layer      | 8.54                   | 87.67 | 1.28    | 11.05    |               |
| TK040608-1               | 10 cm    | Soil           | 20.45                  | 55.92 | 1.83    | 42.25    |               |
|                          |          | Soil           | 12.59                  | 52.70 | 2.41    | 44.89    |               |
| TK040608-2               | 13 cm    | Ash layer      | 20.34                  | 39.65 | 6.47    | 53.99    |               |
| TK040608-3               | 43 cm    | Soil           | 19.27                  | 22.44 | 20.61   | 56.95    |               |
| WK030513-5               |          | Rock River     | 40.86                  | 66.17 | 4.83    | 29.00    |               |
| WK040630-4.83            | 4.83 m   | suspension     | 9.18                   | 7.89  | 5.59    | 86.52    |               |
| U2303 4-6 cm             | 4-6 cm   | Shelf sediment | 38.08                  | 80.55 | 2.43    | 17.02    |               |
| U2303 18-19 cm           | 18-19 cm | Shelf sediment | 6.06                   | 5.54  | 18.82   | 75.64    |               |
| U2303 31-33 cm           | 31-33 cm | Shelf sediment | 38.42                  | 81.27 | 2.30    | 16.43    |               |
| <b>Waiapu Catchment</b>  |          |                |                        |       |         |          |               |
| WU030519-2               |          | Rock River     | 39.18                  | 57.01 | 5.95    | 37.04    |               |
| WU030917-5.40            | 5.40 m   | suspension     | 7.35                   | 6.91  | 7.06    | 86.04    |               |
| TAN0314-31 MC3           | 1-2 cm   | Shelf sediment | 22.62                  | 90.07 | 3.52    | 6.41     |               |
| TAN0314-50 MC10          | 1-2 cm   | Shelf sediment | 10.08                  | 9.05  | 12.55   | 78.39    |               |

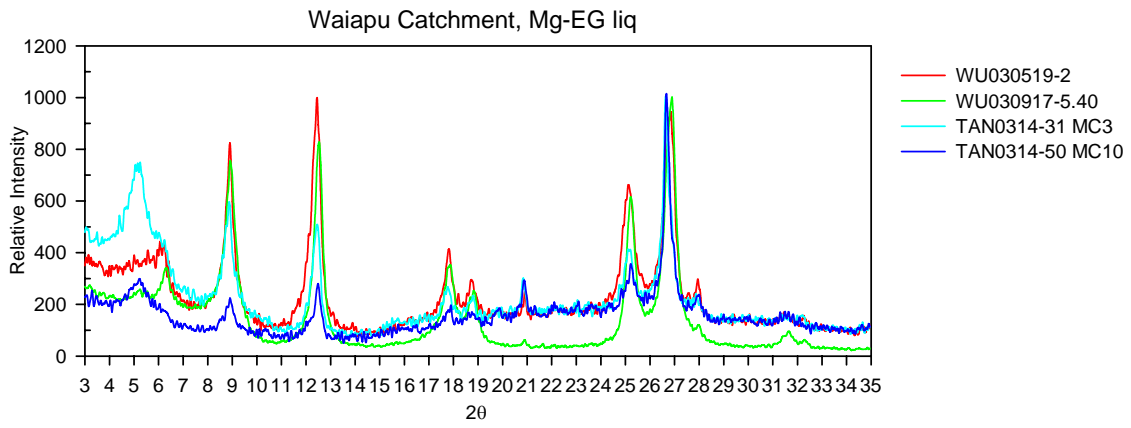
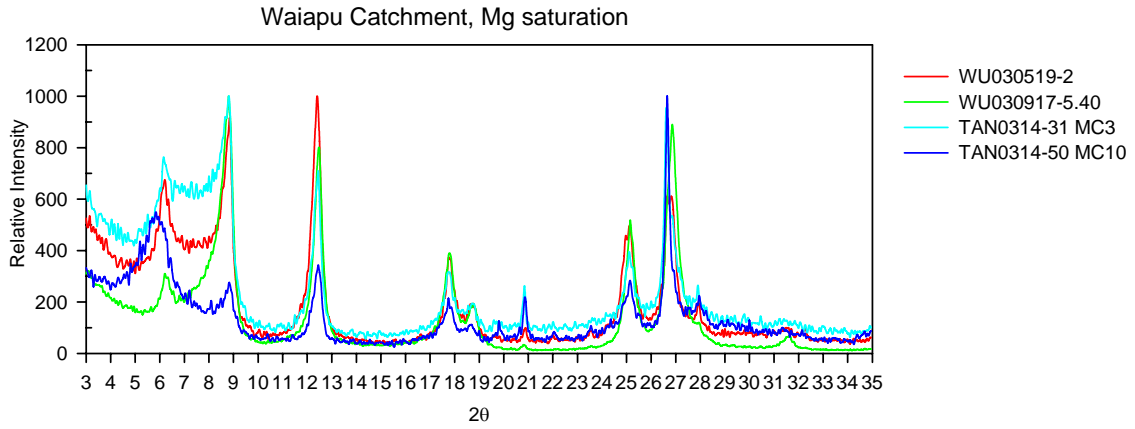
## 7.2 Clay mineral compositions of samples based on Biscaye's method.



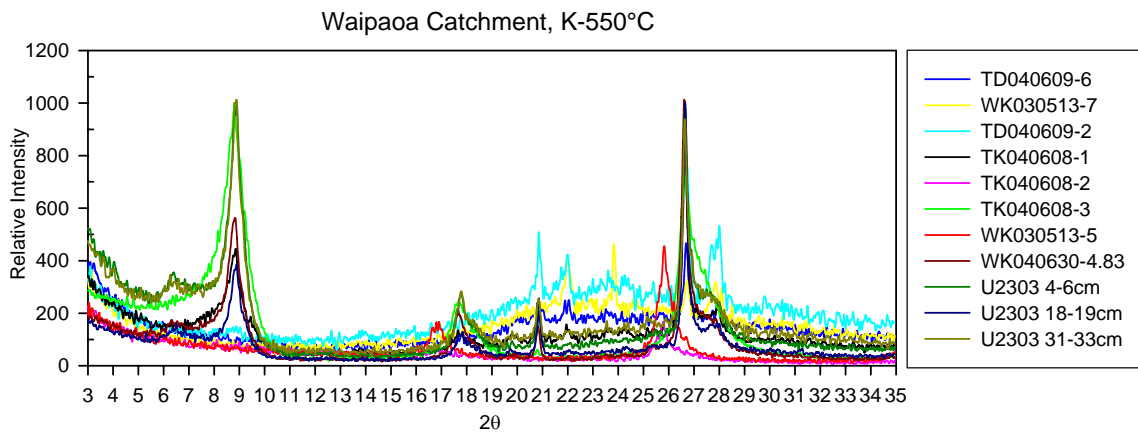
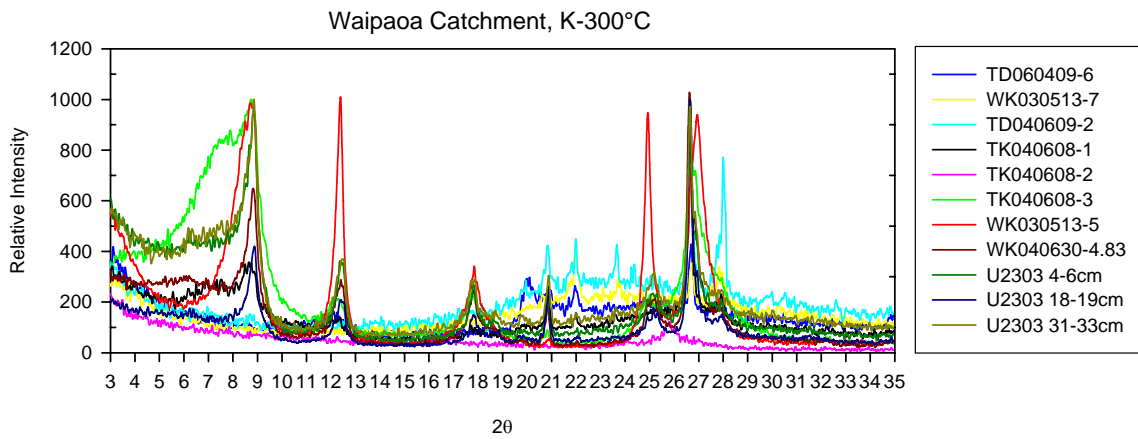
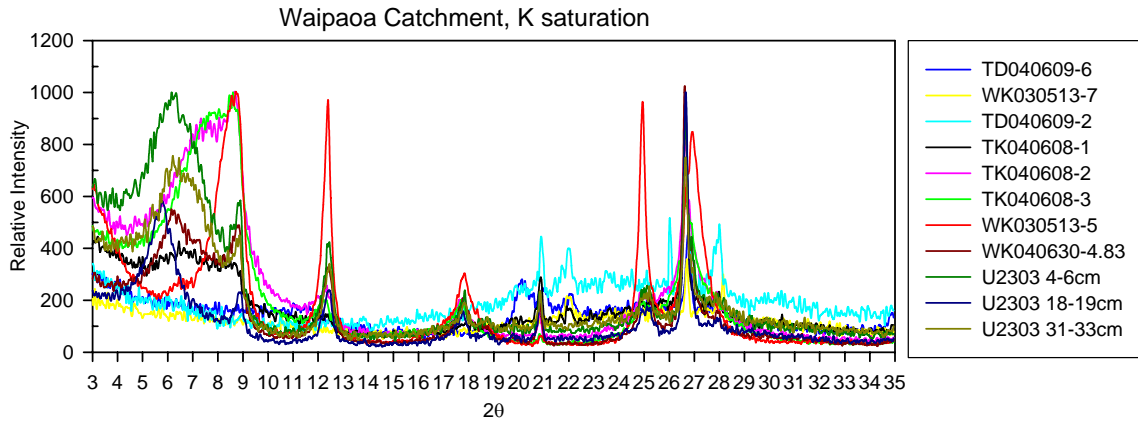
Clay mineral compositions of samples based on Biscaye's method. Tarndale and Whakarau Rd samples contained no characteristic, measurable peaks of crystalline minerals to be quantified using Biscaye's method.

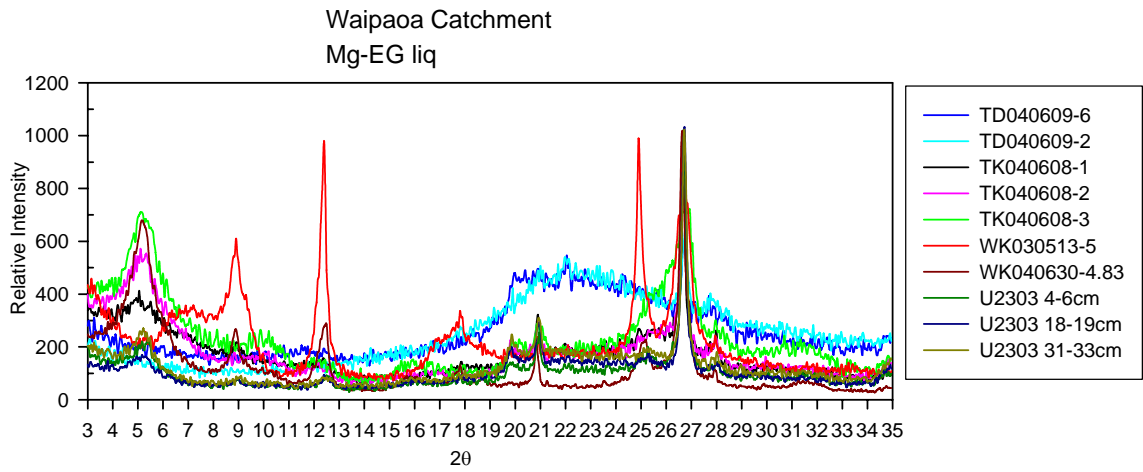
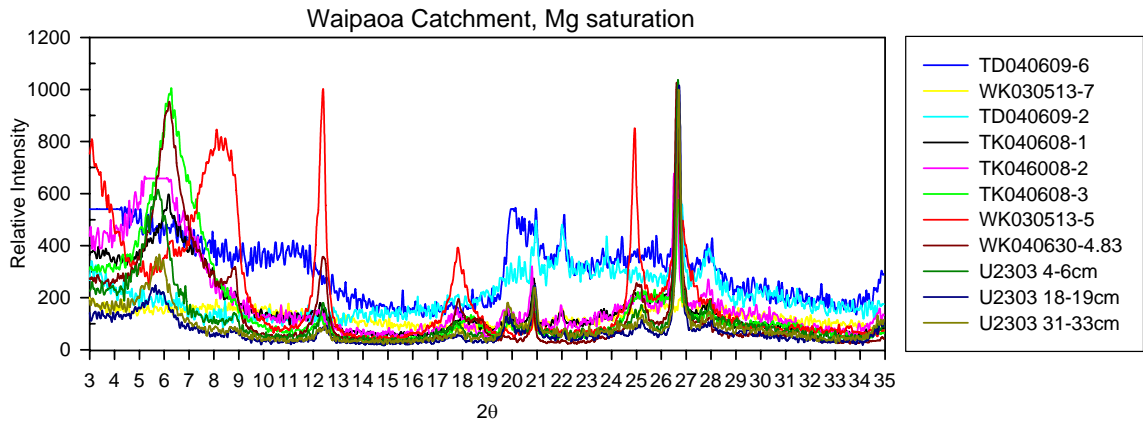
### 7.3 XRD patterns of <2 μm sediment samples for mineralogical analysis



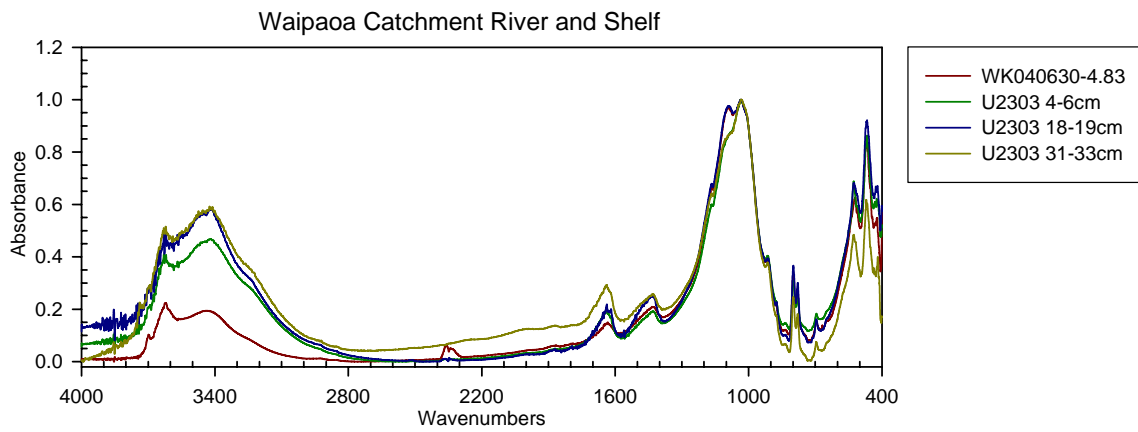
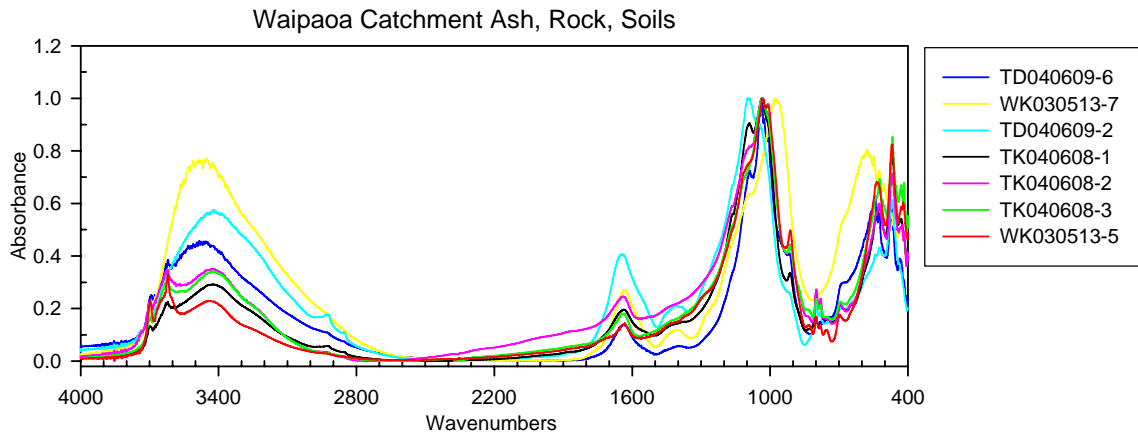


# XRD patterns for Waipaoa Catchment





## 7.4 FTIR spectra of <2 μm sediment samples for mineralogical analysis



## FTIR spectra for the Waiapu Catchment

